Stability improvement to a ruthenium catalyst for partial oxidation of methane

DEPARTMENT OF CHEMICAL ENGINEERING | LUND UNIVERSITY
HULTEBERG CHEMISTRY AND ENGINEERING AB
MELKER AXELSSON | MASTER THESIS | 2022

Stability improvement to a ruthenium catalyst for partial oxidation of methane

by

Melker Axelsson

Hulteberg Chemistry & Engineering AB and
Department of Chemical Engineering
Lund University

December 2022

Supervisor: **Professor Christian Hulteberg**
Co-supervisor: **CTO Per Tunå**
Examiner: **Professor Ola Wallberg**

Picture on front page: Catalyst grains chill at the beach. By author using DALL.E AI Image Generator.

Postal address
P.O. Box 124
SE-221 00 Lund, Sweden
Web address
www.chemeng.lth.se

Visiting address
Getingevägen 60

Telephone
+46 46-222 82 85
+46 46-222 00 00
Telefax
+46 46-222 45 26

Acknowledgements

This project was performed during the autumn of 2022 at Hulteberg Chemistry & Engineering AB and focused on improvements to a catalyst for partial oxidation of methane into syngas.

The support of my supervisor, Christian Hulteberg, is gratefully acknowledged. Thank you for giving me the opportunity to perform this interesting project in which I have learnt lots of useful skills, and for help with interpreting the results and answering lots of theory questions.

Also thank you to Per Tunå, the co-supervisor, for help with the testing equipment and for our many discussions in your office.

Furthermore, many thanks to all my colleagues at Hulteberg who have provided a warm and welcoming atmosphere, as well as help with a myriad of small and big problems along the way.

Melker Axelsson

Lund, December 2022

Abstract

Catalytic partial oxidation of methane (CPOM) is an energy-efficient alternative to steam reforming, the currently prevailing method for energy production from natural gas. Hulteberg Chemistry & Engineering AB has developed a catalyst for the partial oxidation of methane into syngas, for use in solid oxide fuel cells. In its current form, the catalyst rapidly deactivates, causing increased material cost and a need for frequent stopping of the process to regenerate the catalyst. This thesis focuses on improvements to the stability of the catalyst to increase its lifetime and thus commercial viability.

Several new granular catalyst formulations were prepared and tested for activity, selectivity and stability in a lab-scale reactor. All catalysts were supported on magnesia-alumina and used low loadings of ruthenium as the main component of the active phase. Modifications were made to the support by adding magnesium, and to the active phase by doping with platinum or palladium. The activity tests showed that all tested catalysts were active for CPOM, with methane conversion and selectivity towards syngas close to the thermodynamic equilibrium. The activity was virtually unaffected by varying the space velocity from 10,000 to 160,000 h^{-1}. Long-term stability tests found that the addition of 10 wt% magnesium to the catalyst support significantly increased stability, although deactivation continued at a reduced rate even after 100 hours. Through kinetic modelling, a catalyst half-life of 123 hours was determined for the modified catalyst compared to 69 hours for the standard catalyst.

Characterization of the long-term tested catalysts by pulse chemisorption found that the modified catalyst had a surface area of 0.21 m^2/g_{sample}, compared to 0.14 m^2/g_{sample} for the standard catalyst, indicating that addition of magnesium increases stability during the calcination and reduction.

Overall, the increased stability by the addition of magnesium gives a good starting point for further research. Several prepared formulations are yet to be long-term tested and characterized; doing this could result in further improvements to catalyst stability.

Popular science abstract (English)

Natural gas will likely remain an important energy source for years to come, as it is still abundant, cheap and cleaner burning than coal. During the transition from fossil resources into renewable energy, our society depends on natural gas if we want to avoid using coal, a dependence which has become particularly evident during the ongoing war in Ukraine. The main process for turning natural gas into energy is called steam reforming, but there are other processes which may be more energy-efficient and less wasteful in some situations. If energy producers can use these improved processes to reduce environmental impact in the short run, the benefits could be substantial in terms of reduced carbon emissions.

One of the processes being studied is called catalytic partial oxidation of methane, or CPOM, and is the focus of this master thesis. Methane is the main component of natural gas, and partial oxidation means burning the methane with less oxygen than during normal combustion. The product of the combustion is energy and so-called syngas, a mixture of carbon monoxide and hydrogen gas. Syngas can be used for many different applications; for example to make chemicals, or to be used in fuel cells for energy.

To make the process require less energy to initiate, a catalyst is used. Catalysts come in many shapes and sizes, but the catalysts used in this project look like small grains of sand. The grains are speckled all over with ruthenium, a noble metal that helps the gas molecules find and interact with each other. A common problem with catalysts is deactivation – the worsening of catalyst performance over time. Developing catalysts that stay active for longer is therefore very interesting as a research topic, as it reduces the cost of the catalyst and less material is wasted. This thesis focuses on ways to reduce the deactivation while making sure that the catalyst still works for CPOM. New catalysts were made by making educated guesses about what changes to the recipe could make it more stable. The catalysts were then tested in a small-scale reactor where CPOM occurred at conditions similar to in a real fuel cell. Which catalyst did best was decided by looking at the concentration of methane and other gases after the reaction and comparing between catalysts. The catalysts were also examined with a special analysis technique to try to explain how the catalyst properties are different from each other.

In the end, this work found that adding magnesium to the grains helped made the catalyst last almost twice as long, depending on how you count. It was also found that the catalyst with magnesium had a larger surface area than the one without. All the tested catalysts, which included some using different metals together with ruthenium, as well as ruthenium in different concentrations, were active for CPOM, although not all were able to be completely tested as each test took a long time to perform, so it is still unknown how stable they are. More tests are probably needed before the catalyst can be seen as completely stable, but the results give a good starting point for further work.

Populärvetenskaplig sammanfattning (Svenska)

Naturgas kommer sannolikt att förbli en viktig energikälla i många år framöver, eftersom den fortfarande är riklig, billig och brinner renare än kol. Under övergången från fossila resurser till förnybar energi är vårt samhälle beroende av naturgas om vi vill undvika att använda kol, ett beroende som har blivit särskilt tydligt under det pågående kriget i Ukraina. Den huvudsakliga processen för att omvandla naturgas till energi kallas ångreformering, men det finns andra processer som kan vara mer energieffektiva och som har minskad resursanvändning i vissa situationer. Om energiproducenter kan använda dessa förbättrade processer för att minska miljöpåverkan på kort sikt kan fördelarna bli betydande i form av minskade utsläpp av växthusgaser.

En av processerna som studeras kallas katalytisk partiell oxidation av metan, eller CPOM, och är fokus för denna masteruppsats. Metan är huvudkomponenten i naturgas och partiell oxidation innebär att man bränner metanet med mindre syre än vid normal förbränning. Produkten av förbränningen är energi och så kallad syngas, en blandning av kolmonoxid och vätgas. Syngas kan användas för många olika applikationer; till exempel för att tillverka kemikalier, eller för att användas i bränsleceller som energi.

För att få processen att kräva mindre energi för att starta används en katalysator. Katalysatorer finns i många former och storlekar, men katalysatorerna som används i detta projekt ser ut ungefär som små sandkorn. Kornen är spräckade med rutenium, en ädelmetall som hjälper gasmolekylerna att hitta och interagera med varandra. Ett vanligt problem med katalysatorer är deaktivering – försämring av katalysatorprestanda över tid. Att utveckla katalysatorer som håller sig aktiva längre är därför mycket intressant som forskningsämne, eftersom det minskar kostnaden för katalysatorn och gör att mindre material går till spillo. Denna uppsats fokuserar på sätt att minska deaktiveringen samtidigt som man ser till att katalysatorn fortfarande fungerar för CPOM. För att åstadkomma detta skapades nya katalysatorer genom att göra välgrundade gissningar om vilka ändringar i receptet som skulle kunna ge mer stabilitet. Katalysatorerna testades sedan i en småskalig reaktor där CPOM skedde under förhållanden liknande en riktig bränslecell. Vilken katalysator som klarade sig bäst bestämdes genom att titta på koncentrationen av metan och andra gaser efter reaktionen och jämföra mellan katalysatorerna. Katalysatorerna undersöktes också med en speciell analysteknik för att försöka förklara hur katalysatoregenskaperna skiljer sig från varandra.

I slutändan visade detta arbete att tillsats av magnesium till kornen gjorde att katalysatorn höll nästan dubbelt så länge, beroende på hur man räknar. Katalysatorn med magnesium hade också större yta än den utan. Alla de testade katalysatorerna, som inkluderade några som använde olika metaller tillsammans med rutenium, såväl som rutenium i olika koncentrationer, var aktiva för CPOM, även om inte alla kunde testas fullständigt eftersom varje test tog lång tid att utföra. Det krävs förmodligen fler tester innan katalysatorn kan ses som helt stabil, men resultaten ger en bra utgångspunkt för vidare arbete.

Table of contents

1 INTRODUCTION 1

1.1 AIM 1

2 LITERATURE SEARCH 2

2.1 REACTIONS 2
2.2 CATALYST FORMULATION PRINCIPLES 3
2.2.1 FUNCTION AND COMPOSITION 3
2.2.2 SYNTHESIS 4
2.2.3 DEACTIVATION 4
2.3 PROMISING CATALYST MODIFICATIONS 5
2.4 TESTING AND OUTLET GAS ANALYSIS 6
2.4.1 GAS CHROMATOGRAPHY (GC) 6
2.4.2 NDIR GAS ANALYZER 6
2.5 CATALYST CHARACTERIZATION 7
2.5.1 CHEMISORPTION 7
2.5.2 TEMPERATURE-PROGRAMMED REDUCTION (TPR) 8

3 METHOD 9

3.1 FORMULATION 9
3.2 TESTING 10
3.2.1 REACTOR AND RIG CONSTRUCTION 11
3.2.2 REDUCTION OF CATALYST 12
3.2.3 ACTIVITY TESTS 12
3.2.4 LONG-TERM PERFORMANCE TESTS 13
3.3 CHARACTERIZATION 13
3.3.1 TPR 13
3.3.2 CHEMISORPTION 13

4 RESULTS AND DISCUSSION 14

4.1 ACTIVITY TESTS 14
4.1.1 CHANGING REACTOR CONDITIONS 16
4.2 LONG-TERM PERFORMANCE TESTS 18
4.3 DATA RELIABILITY 20
4.4 KINETIC MODELING OF DEACTIVATION 21
4.5 CHARACTERIZATION RESULTS 23
4.5.1 PULSE CHEMISORPTION 23
4.5.2 TEMPERATURE PROGRAMMED REDUCTION (TPR) 24

5 CONCLUSION 26
6 REFERENCES 27
7 APPENDICES 29

7.1 APPENDIX A: LIST OF PREPARED CATALYST RECIPES 29
7.2 APPENDIX B: CONVERSION CALCULATION FOR LONG-TERM TESTS 30
7.3 APPENDIX C: DERIVATION OF KINETIC MODEL 32
7.4 APPENDIX D: SUPPORTING IMAGES 33

1 Introduction

Despite its environmental drawbacks, the global dependence on natural gas remains substantial, with gas currently satisfying 22.5% of the world's energy demand, its production nearly double that of twenty years ago.[1] While long-term investments into sustainable energy sources are clearly necessary, improvements of natural gas technologies can provide emission reduction in the short term through increased energy efficiency. A viable use for natural gas is the production of syngas, from which higher valued chemicals can be synthesised through the Fischer-Tropsch process, or used as fuel in a solid oxide fuel cell (SOFC), for example. The most common process for syngas production from natural gas is steam reforming (SR), but it is endothermic, requiring an initial heating of the reactor. Conversely, catalytic partial oxidation of methane (CPOM), the subject of this work, is exothermic and yields syngas with an H_2/CO ratio of 2, ideal for Fischer-Tropsch applications.[2] Unlike SR, the addition of steam is not required, making it a highly flexible technology with short start-up and shut-down times, useful for situations where flexible power generation is needed. One potential application is as an auxillary power supply to intermittent renewable energy production, such as wind and solar, where it could be automatically switched on during periods of power shortages to stabilize energy generation.

Nickel catalysts have previously been used for SOFC. These, however, cause substantial coking (carbon formation) on the surface of the anode.[3] There is therefore an interest in creating catalysts with higher stability and a lower tendency for coking. Such improvements are the focus of this work, with new catalysts being formulated, tested and characterized.

1.1 Aim

Hulteberg Chemistry & Engineering AB has developed a CPOM catalyst for application in solid oxide fuel cells. The application requires the catalyst to be active for at least 100 hours, however in its current form suffers from heavy deactivation by coking and sintering, limiting its lifetime to around 30 hours. The aim of this work is to investigate improvements to the catalyst formulation to reduce deactivation while maintaining high methane conversion and a suitable product stream composition during the desired timeframe. To achieve this, new catalyst formulations are prepared with support from literature, and the catalysts are tested and evaluated for their performance in terms of methane conversion and catalyst deactivation.

The project was carried out in four phases:

1. Literature phase: understanding catalyst functionality and finding suitable modifications
2. Formulation phase: synthesizing new catalysts based on the literature
3. Testing phase: evaluating catalyst performance in a lab-scale reactor
4. Characterization phase: examining physical and chemical properties of the catalysts by chemisorption

2 Literature search

In this section, the reactions involved in CPOM are explained. The function, general manufacturing principles and deactivation mechanisms of the granular catalysts investigated in the report is given. A literature review is carried out resulting in proposed catalyst modifications. The principles of catalyst testing and some useful characterization methods are also presented.

2.1 Reactions

The reactions involved in CPOM are shown in Table 2.1. The overall partial oxidation of methane reaction (R1) consists of an exothermic total oxidation (R2) in which all oxygen is consumed, followed by a system of reactions (R3-R5), which together determine the equilibrium composition.[4] While the total oxidation is near instantaneous, the subsequent reactions (R3-R5) are slow as the simultaneous adsorption of both reactants to the catalyst surface is required. As endothermic reactions, R3-R5 are thermodynamically favoured at higher temperatures, meaning that selectivity towards hydrogen and carbon monoxide increases with the temperature. At lower temperatures, the time required for these reactions to occur is insufficient and the main products will be CO_2 and water, with some H_2 possibly forming through the water-gas shift.

Table 2.1: Reactions involved in the partial oxidation of methane.

Name	**Reaction formula**	ΔH^0_{298} **(kJ/mol)**	
Partial oxidation	$CH_4 + \frac{1}{2}O_2 \rightarrow CO + 2H_2$	-36	(R1)
Total oxidation	$CH_4 + 2O_2 \rightarrow CO_2 + 2H_2O$	-802	(R2)
Steam reforming	$CH_4 + H_2O \rightleftharpoons CO + 3H_2$	206	(R3)
Dry reforming	$CH_4 + CO_2 \rightleftharpoons 2CO + 2H_2$	247	(R4)
Water-gas shift	$CO + H_2O \rightleftharpoons CO_2 + H_2$	-41	(R5)

The theoretical equilibrium composition can be predicted using process simulation software such as ASPEN Plus ®. Such a simulation was performed for CPOM, and is shown in Figure 2.1. This way, the activity of the catalysts can be compared against the theoretical maximum conversion.

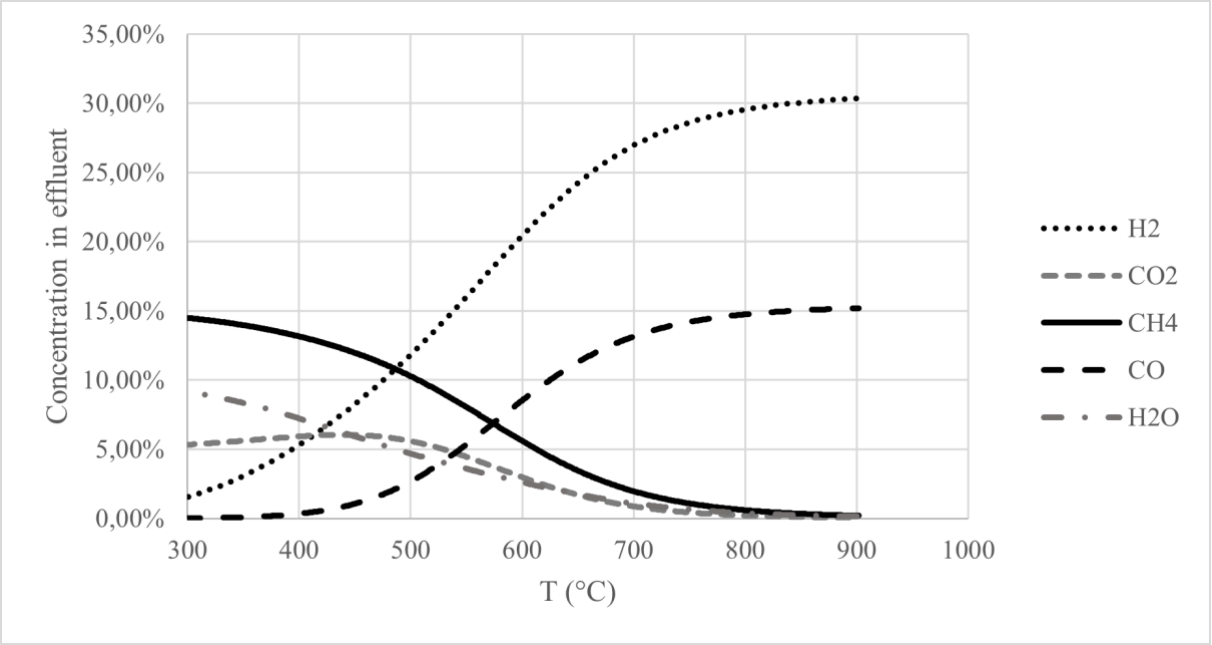

Figure 2.1: ASPEN simulation of outlet concentrations at varying reaction temperatures, given an inlet concentration of 20% CH_4, 10% O_2 and 70% N_2 by volume flow. P = 1 bar.

2.2 Catalyst formulation principles

Here, important catalysis concepts are explained. The manufacturing process and deactivation mechanisms are also presented.

2.2.1 Function and composition

Generally, heterogeneous catalysts consist of three main components: *carrier*, *support* and *active phase*. Like a skeleton, the carrier makes up the structure of the catalyst, giving it shape and determining heat and mass transfer and pressure drop, important reaction parameters. The macrostructure of the catalyst carrier can be tailored to the application with monoliths and granulates being two common forms. Granular carriers are small, porous, sand-like grains of a specific size which are packed into the reactor, forming a bed into which reactants diffuse. Monoliths are oblong structures with fixed, identical passages that the reactants pass through, commonly made from ceramic or metal materials.

For a catalytic reaction to proceed efficiently, a large surface area is required. This is provided by the catalyst support, which is made from highly porous materials like alumina, ceria or silica. In some cases, the support and carrier are made from the same material, and may even be functionally indistinguishable. When the support is applied to the carrier, the total surface area can be in the scale of 100 m^2/g, although mass transfer limitations mean that the whole area is unlikely to be available during a reaction.

The active phase consists of particles of either metals or metal oxides which are dispersed across the catalyst surface. These contain sites on which the reaction takes place. An important design rule for the active phase is the Sabatier principle, which states that the active phase should have a strong affinity with the reactants, i.e. interact with the reactants enough for them to adsorb, but the interaction must not be too strong, since otherwise the products cannot desorb

and remain on the surface as a catalyst poison. Transition metals like Ni, Fe, Cu, Pt, Ir, Ru and Rh have this property and are therefore used extensively in heterogeneous catalysis.

In addition to the main three components, promoters and binders may be added to improve catalyst performance in various ways. Promoters are often based on industry trial and error, and may be added to enhance the properties of the catalyst by increasing activity or limiting side reactions. It may also have a synergetic effect with the main active phase metal by being catalytically active for a different step in the reaction mechanism.[5] Binders are added to increase adhesion between support powder particles, resulting in larger, granular catalysts that can be used in a reactor.

2.2.2 Synthesis

The starting point for the synthesis of granular catalysts is the support material powder. Catalysts in powder form are too small and light to be used in the reactor on their own, so the transformation of the powder into larger particles is required. This is done by adding a binder material to the powder, and drying and calcining (heating to high temperature, with a reaction occurring) the mixture. The resulting hard cake is then ground and sieved into an appropriate size. Each active component (promoters and active phase) is then added onto the support one by one in a certain order. Between each component, the catalyst is dried and then calcined which stabilizes the component so that its microstructure transforms into the desired one and does not change during the reaction.

In all coating steps, it is important to ensure an even distribution of the component on the support surface, as several problems may otherwise arise. Uneven distribution of binder will cause some of the catalyst particles to be very hard and difficult to grind into smaller grains, while others remain in powder form and are unusable in the reactor. Uneven distribution of promoters and active phase means that some catalyst particles will be significantly more active than others, potentially resulting in hotspot formation or extensive local deactivation, as well as loss of available active sites due to active phase clustering.

A technique that achieves a good dispersion of coated material is the *incipient wetness* technique. Its principle is that if the support is impregnated with a liquid volume exactly the same as the total pore volume (which can be measured), capillary forces will ensure that the liquid and any dissolved substances (e.g. active phase) are distributed reasonably evenly in the passages and canals of the support particles. During oven drying, the water evaporates and the coating material remains on the surface of the support. Because all the liquid was absorbed we can be sure that all the coating material has entered the particles, and we simultaneously know that enough solution was added to fill the pores completely without any dry areas. In practice, the water absorption capability of the support is measured by adding water to a sample of support until visible saturation. The total pore volume of the support can then be calculated, and a solution containing the right amount of coated material is prepared and mixed with the granular catalysts. The catalyst is then dried and calcined which removes the water and affixes the coated material to the support.

2.2.3 Deactivation

Catalyst lifetime is limited by deactivation through three mechanisms: sintering, coking and poisoning. Sintering is the gradual migration and agglomeration of metal particles, caused by high temperature, long exposure time and weak metal-support interaction. As the metal particles form clusters, the share of metal area exposed to the surface decreases, leading to an overall

decrease in activity. Sintering can be prevented by strengthening the interaction between active phase and support through modification of the support properties.

Coking is the deposition of carbon onto the catalyst surface. The deposited carbon can block catalyst pores, making the active phase inside unavailable, or deposit directly on the active phase, decreasing the activity of the catalyst. Coking is promoted if hotspots are present in the reactor (poor heat transfer), and by the presence of acidic groups on the catalyst surface. Reactor design and support properties are therefore important factors for limiting coking.

Poisoning is caused by the presence of unwanted compounds, for example by sulfur which may be present in natural gas, in the reaction system. Poisoning is not addressed in great depth in this work, as pure reactants are used, and the effect of sintering and coking are expected to be more significant. It is, nevertheless, a challenge for CPOX in fuel cell applications.[6]

2.3 Promising catalyst modifications

A literature search was performed to provide a basis for new catalyst formulations. The most common choice for active phase is nickel, which has been used extensively because of its low price (26 €/kg).[7] However, while cheap, Ni catalysts come with several drawbacks, the most important ones being significant coking and weak interaction with the support material, leading to sintering. In contrast, noble metals like Pt, Rh and Ru have high activity, low coking which may compensate for their high cost, causing much research interest. Among the noble metals, Ru is the cheapest at 19200 €/kg[8], and is therefore of special interest.[2]

The properties of the support material also have a great impact on the activity of the catalyst. Lanza et al.[9] investigated three Ru catalysts supported on ceria-zirconia, silica and alumina, respectively. The results showed that ceria-zirconia gave a low selectivity towards syngas, and silica is quickly deactivated. Alumina on the other hand showed high activity with some stability problems, making it an attractive candidate for further studies.

Another interesting class of supports, used in previous tests by Hulteberg, are hydrotalcites which are layered carbonate minerals with the formula $Mg_6Al_2CO_3(OH)_{16}\cdot 4H_2O$. These are advantageous because they form spinel structures upon calcination, which have large specific surface areas, strong interaction between the support and active phase, and good dispersion of the active phase.[10] Furthermore, the basicity of the support can be tuned by varying the ratio between the metals; e.g. increasing Mg/Al ratios resulted in less deactivation by carbon deposition in experiments on Ni-Au catalysts by Maniecki et al.[11]. Previous results by Hulteberg have suggested that binder acidity is a likely cause for deactivation, making this tunable basicity property especially interesting; increasing the pH may lead to fewer acid seats in the completed catalyst. Varying the Mg/Al ratio has not, to the author's knowledge, been tested previously for Ru catalysts for the POM reaction, making it an interesting choice for modifications to the catalyst formulation.

The addition of promoter metals can give the catalyst certain advantages. Previous results have shown that adding Pt to an Ru catalyst gave a stabilizing effect, with Pt possibly acting as an anchor for Ru, resulting in reduced sintering through the formation of volatile RuO_4.[12] Pd has also been used as a promoter metal, allowing the partial oxidation reaction to start at 50 degrees lower than for an Ru-only catalyst.[5] Because sintering is temperature dependent, this could lead to a more stable catalyst. Adding small amounts of Pt or Pd are therefore interesting ideas for the formulation of new catalysts.

Finally, the temperature at which the support material is calcined affects its microstructure and could result in fewer acid seats forming.

Based on these findings, new catalyst formulations were chosen, prepared and tested for their performance in terms of activity, product selectivity and stability.

2.4 Testing and outlet gas analysis

The activity, selectivity and stability of the prepared catalysts can be evaluated by performing the reaction in a lab-scale reactor and analyzing the outlet gas. Two sets of equipment were used for this throughout the testing phase of the project. A gas chromatograph (GC) was used for the first part, and a non-dispersive infrared sensor (NDIR) was used for the second. Given below are descriptions of the working principles of these analysis methods and some important practical aspects.

2.4.1 Gas chromatography (GC)

Gas chromatography (GC) coupled with a detector is a common method for separating and analyzing a sample containing several different compounds. The analyte mixture is injected into the GC port together with an inert carrier gas (N_2 in this case), and travels through a column packed with silica or another polar material. In the column, the compounds interact with the packing material and the strength of the interaction determines the degree of separation. Compounds with strong interaction will have a longer retention time (i.e. take longer time to exit the column) than compounds with weak interaction and this retention time is used to identify the compound. The amplitude of the signal as the compound reaches the detector is plotted against the elution time of the compound and a spectrum of peaks is obtained, with each peak corresponding to an analyte. The area of a peak compared to the total area is the concentration of the corresponding analyte, and the concentration of each compound can therefore be determined with high precision.[13]

The GC used at Hulteberg (*Scion 456-GC*) is equipped with three detectors: two thermal conductivity detectors (TCD) for measuring CH_4, CO, CO_2, H_2, O_2, and N_2, and one flame-ionization detector (FID) which measures CH_4. For the experiments conducted in this report, the reported results are from the TCD. TCDs measure the ability of a substance to transfer heat from a hot area to a cold area (thermal conductivity), which is characteristic for each substance. It is important that the carrier gas has a distinctly different thermal conductivity than the analytes to avoid overlap; for this reason, helium is used as the carrier gas. The sensitivity of the TCD is inversely proportional to the flow rate, meaning it is important to limit the flow from the reactor to the GC to ensure an accurate result.[14] The measurements of gases at high concentration, i.e. N_2 and H_2, will therefore be less accurate than the measurements for CH_4, CO and CO_2. Another important measurement aspect, which applies to the NDIR analyses as well, is the equilibration time. The reactor requires some time to reach and stably maintain the correct temperature and the reaction needs some time to reach equilibrium. Finally, the gas requires some time to travel from the reactor to the analysis instruments. It was found in the experiments that there should be a buffer period of at least 15 min between increasing the oven temperature and taking the GC measurement.

2.4.2 NDIR gas analyzer

Also connected to the reactor equipment was a *Sensors inc. Gasmitter* gas analyzer equipped with an infrared light (IR) detector, able to quantify the CH_4 content (as a percentage of the

total flow) of a stream with a precision of $\pm$0.2%. The gasmitter was used instead of the GC for part of the project (the long-term tests) due to external circumstances. Since it measures concentrations in real time unlike the GC, it was also used to determine whether equilibrium had been reached before starting the GC measurements. The apparatus measures light absorbance at a characteristic wavelength which is unique for each bond type present in the analysis gas. The type and quantity of each bond can be identified from the resulting absorption spectrum and translated into a stream concentration.[14] The gasmitter is able to measure continuously but because the low precision will cause some measurement noise, it is best to measure in short time intervals and average the data to obtain a measurement with high accuracy. Nevertheless, the quantitative results of the gasmitter will be less precise than those of the GC.

2.5 Catalyst characterization

While testing gives information about the activity and stability of the catalyst, further analyses can be made to determine their physical and chemical properties. The analyses can be used to explain phenomena observed during the testing phase of the project. Below follows descriptions of the techniques used in this project for catalyst characterization.

2.5.1 Chemisorption

Active sites allow molecules to adsorb to their surface where the reaction takes place. By exposing the catalyst to a known volume of reactive gas, and measuring the difference at the outlet, the volume of adsorbed gas on the catalyst surface can be obtained. From this, many interesting catalyst properties can be determined. Chemisorption with CO or H_2 can give information about the surface area and degree of dispersion of the active metal, which are properties related to catalyst activity. Differences observed between used catalysts can help explain deactivation behaviors during the testing phase, and differences between fresh catalysts can give information about sintering from the calcination during the formulation phase. Additionally, chemisorption using NH_3 can give the number of acid sites of the sample which would be interesting since acid sites are believed to be the cause of the deactivation in the current Hulteberg catalyst.

There are two methods of carrying out chemisorption; *static* and *dynamic*, described in detail by Fadoni and Lucarelli[15]. Static chemisorption involves injecting a known volume of adsorbate and gradually increasing the system pressure until a complete monolayer of adsorbate is formed on the surface. From the resulting isotherm the total chemisorbed volume can be determined. With the static method, physisorption, weak and strong chemisorption can be calculated separately, but the analysis is slow and requires the maintenance of vacuum in the system without gas leakage.

A common dynamic method is pulse chemisorption, which consists of continuously flowing inert gas over the sample and introducing pulses of reactive gas. At each pulse, some of the active sites will be filled, and the rest of the gas volume exits the system and is quantified. The pulse is repeated until saturation of the catalyst surface. The inert flow continuously removes the physisorbed and weakly chemisorbed gas molecules, meaning that the dynamic method only measures strongly adsorbed species. Pulse chemisorption is much faster than static at around 2-3 hours.

The reactive gas needs to be chosen based on the active phase metal. For ruthenium, H_2 may be used, although the equilibrium is reported to be very slow[16], making it potentially difficult

to use for dynamic analysis. CO on the other hand can be used for both methods. CO chemisorbs associatively (i.e. without dissociating into free C and O atoms on the surface) and depending on which orientation it adsorbs with, the estimation of the surface area will vary. Fortunately, the adsorption is site-specific and association happens the same way each time, meaning that area estimations for different catalyst samples can be qualitatively compared without having to investigate the orientation of the molecule upon adsorption. The stoichiometry of CO on Ru chemisorption, i.e. the number of CO molecules adsorbed per Ru atom, is known to be 1:1, however.[15]

2.5.2 Temperature-programmed reduction (TPR)

In TPR, diluted H_2 is flowed over the sample under increasing temperature, eventually completely reducing the catalyst, and the difference in quantity of inlet and outlet H_2 flow is measured.[15] The main purpose of TPR is to determine the temperature at which the active phase is reduced, and more specifically: the lowest possible temperature for complete catalyst reduction. Maintaining a low temperature is useful to prevent unnecessary sintering, and thus increasing catalyst lifetime.

3 Method

20 catalyst formulations were prepared by incipient wetness impregnation. Six of these were tested for CPOM activity at 500-700 °C in a lab-scale reactor. Two catalysts were stability tested at 600 °C for 100h. Fresh and spent samples of the stability tested catalysts were characterized by pulse chemisorption. Some supporting images are available in 7.4.

3.1 Formulation

The catalyst preparation consisted of four steps, the specifics of which were varied to investigate the findings from the literature search:

1. Calcining of support material.
2. Addition of boehmite (binder), followed by drying and calcining.
3. Addition of magnesium (promoter), followed by drying and calcining.
4. Active phase and additional promoter impregnation, followed by drying and calcining.

Here follows the standard recipe for the catalyst formulation (i.e. C1). The support material *Sasol Pural MG30*, a powder consisting of 30 wt% magnesia and 70 wt% alumina, was calcined in an electrical furnace at 850 °C for 4 h. 50 g of MG30 was used per catalyst formulation.

Nyacol AL20, a colloidal dispersion of boehmite (alumina) was mixed with a suitable amount of water, determined by a water uptake measurement until incipient wetness, and then mixed with the powder on a tray. The amount of boehmite added was 20% of the weight of the support. The mixture was then dried at 120°C for 4h and calcined at 850 °C for 4 h, which phase transforms boehmite into δ-alumina. The resulting hard cake was ground and sieved to a size range of 840-1680 μm (mesh size 10-20).

The impregnation of 2% Ru by total granulate mass was done by mixing *Umicore* $RuCl_3$ solution (20.46 wt% Ru) with the appropriate amount of water according to a water uptake measurement, and dripping the stirred solution onto the particles with a pipette, aiming for an even distribution of active phase across the granulate surface. The impregnated granulates were then dried at 120 °C for 4 h and calcined at 500 °C for 4 h.

Based on the findings of the literature search, modifications to the standard recipe were carried out. The first modification was the impregnation of 1-10 wt% of magnesium between the boehmite addition and the active phase impregnation. This was done by mixing *Umicore* magnesium nitrate, with water according to a water uptake measurement. The stirred solution was then dripped onto the catalyst particles in the same manner as for the active phase impregnation. The impregnated granulates were then dried at 120 °C for 4 h and calcined at 850 °C for 4h.

The second modification was of the active phase, with the addition of Pd and Pt as support. This was done as co-impregnation (i.e. mixing the metal solutions and dripping them onto the granulates as in the standard case, except for one case, where serial impregnation of Pt followed by Ru was done, with a calcining step in-between, in order to investigate the anchoring effect of Pt found in the literature search.

For the last modification, the literature search found that increasing the calcining temperature of the support material could have beneficial results. Therefore, two such catalysts were prepared by calcining MG30 at 900 and 950 °C, respectively.

In total, 8 catalyst recipes, summarized in Table 3.1, were prepared and tested. An additional 12 catalysts, which were not tested, were also prepared. 7.1 lists a complete summary containing all prepared catalysts for future reference. The varied parameters in the catalyst formulation are labeled into three series. The catalysts where magnesium was added are labeled *CS*; the ones with a modified active phase are named *CA* and the catalysts with varied support material calcination temperature are named *CK*. The reference catalyst is named *C1*. After initial testing, a second batch of catalysts with 0.5% Ru as a standard was prepared. Catalysts from this batch have the prefix *β*-.

Table 3.1: Summary of the tested catalyst formulations. All given percentages are weight-based (wt%).

Name	Support material	Support calcining temperature (°C)	Added Mg	Active phase
C1	MG30	850	0%	Ru (2%)
CS4	MG30	850	10%	Ru (2%)
CA1	MG30	850	0%	Ru (1%)
CA2	MG30	850	0%	Ru (2%), Pd (0.5%)
CA3	MG30	850	0%	Ru (2%), Pt (0.5%)
CA6	MG30	850	0%	Ru (2%), Pt (0.5%), impregnated in series
β-C1	MG30	850	0%	Ru (0.5%)
β-CS4	MG30	850	10%	Ru (0.5%)

3.2 Testing

To test the performance of the catalysts, a lab-scale reactor was constructed and placed in a ventilated 'rig' equipped with mass flow-controlled gas inlets and an oven for heating. All catalysts were activated through reduction with diluted H_2 at 400°C for at least 4h. The catalysts in the first batch (C1, CS4, CA1, CA2, CA3, CA6) were tested for their performance in short-term temperature ramp activity tests. The outlet gas stream concentrations were determined in a gas chromatograph (GC) equipped with a thermal conductivity detector (TCD). Methane conversion and product selectivities could then be calculated (see Calculations). Long term performance tests of the second batch (β- series) were later carried out to determine catalyst stability. Due to circumstantial limitations, the GC could not be used at this point in the project, and so the long-term tests used a *Sensors-inc.* brand non-dispersive infrared (NDIR) *Gasmitter* equipped with a methane TCD. The long-term stability in terms of methane conversion decay over time could then be evaluated.

An important parameter for the testing is the gas hourly space velocity (GHSV) which is the ratio between the volumetric flow rate at STP (0 °C, 1 atm) and the total catalyst particle volume (eq. 1).

Gas hourly space velocity:

$$GHSV = \frac{\dot{V}}{V_{cat}} \quad (1)$$

Increasing the GHSV lowers the methane conversion as the reactant surface contact time is decreased. During testing, maximum conversion is not desired as the difference in activity between the catalyst will not be shown. GHSV should therefore be chosen so that conversion is around 75% of the maximum conversion. In theory, this can also be done by reducing the volume of the catalyst bed, but in practice it is better to increase the reactant flow, as changing the catalyst volume has other effects, such as temperature gradient formation and increased pressure drop which affect the results.

3.2.1 Reactor and rig construction

A lab-scale packed bed tube reactor was constructed from scratch using pipes and connectors, according to the schematic in Figure 3.1. The reactor chamber was sealed at each end with quartz wool at the bottom to prevent catalyst particles from falling out. The preheater chamber was packed with inert alumina balls to increase reactant gas mixing and heat transfer. In preparation for each test, the reactor chamber was filled with 2 ml of catalyst granulates and 20 ml of inert material (α-alumina), after which the reactor was sealed. Before sealing, metal paste was coated onto the pipe connection to prevent soldering and thus increase the lifetime of the reactor. The temperature at the catalyst bed inlet and middle were measured with two thermometers placed with the tips at the radial centers of the bed. The reactor was placed in a ventilated chamber (*rig*) equipped with a partitioned electrical oven and fittings for inlet and outlet gas connections. The reactant gases were connected to the rig along with mass flow controllers (MFCs) for CH_4, N_2, air and reduction gas (4% H_2 in N_2). The volumetric flows and oven temperatures were controlled through a connected computer.

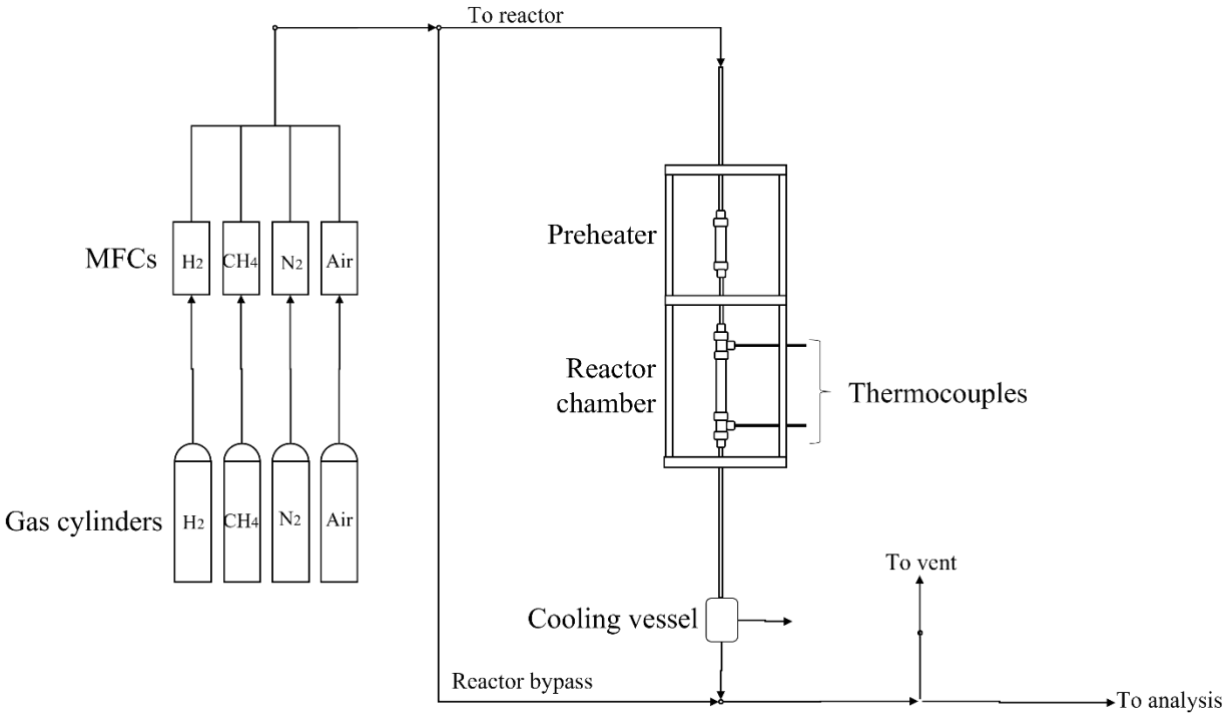

Figure 3.1: Schematic of rig setup. MFC = mass flow controller.

3.2.2 Reduction of catalyst

After formulation, the active phase of the catalyst is in its oxide form, (i.e. RuO_2) which is catalytically inactive. Before starting the tests, the catalysts were therefore activated through reduction with diluted hydrogen at 400 °C for at least 4 h, which ensured the complete reduction of the surface.

3.2.3 Activity tests

To determine the activity and product selectivity of the catalysts, temperature ramp activity tests were performed at 400-700 °C with an inlet gas composition of 10% O_2, 20% CH_4 and 70% N_2 and with varying GHSV, starting at 10,000 h^{-1} which corresponds to a total gas flow of 20 L/h. The inlet composition was based on the stoichiometry of the CPOM reaction, with added nitrogen as dilution to prevent temperature runaway and hotspot formation. The outlet gas was analyzed using a *Scion* brand GC and detected by a TCD. From the resulting gas composition, the conversion of methane and the product selectivities were calculated (see Calculations). Bypass measurements were performed to verify the composition of the unreacted gas and use as reference for the calculations. Each MFC has a specific operating flow rate, so when the flow rate had to be increased beyond this in the later part of the experiments, the MFCs had to be swapped. New bypass measurements were made after each swap to ensure consistency of the reactant gas composition. Catalyst reduction was performed, after which reactant flow was started, and the oven temperature was adjusted to reach the desired temperature. After waiting for the reactor bed temperature to stabilize, the stabilization of the reaction itself was checked with the Gasmitter which continuously measured the effluent concentration of CH_4, after which a GC injection was made. After injecting, the oven temperature was increased, and the measurement was repeated for the desired temperatures.

Calculations

Catalyst activity was determined in terms of CH_4 conversion and CO and H_2 selectivity. CH_4 *conversion* was defined as the ratio between reacted and inlet CH_4 flow (eq. 2). The *selectivity* of a component was defined as the component outlet flow divided by the total outlet product flow (eq. 3).

Conversion of methane:
$$x_{CH4} = \frac{F_{CH4,in} - F_{CH4,out}}{F_{CH4,in}} = 1 - \frac{F_{CH4,out}}{F_{CH4,in}} \quad (2)$$

Selectivity of product A:
$$S_A = \frac{F_{A,out}}{\sum_{i=1}^{n} F_{i,out}} \quad (3)$$

As the reaction will cause a volume change, and the GC only measures the effluent gas concentrations, it becomes necessary to calculate the total flow after the reaction in order to calculate the conversion. However, as N_2 is inert, its flow will be unchanged during the reaction, the GC measured concentration can be used to calculate the total flow (eq. 4). The flow of each component can then be calculated as the total flow times the GC measured concentration (eq. 5), assuming total conversion of oxygen.

Total outlet flow:
$$F_{tot,out} = \frac{F_{N2,in}}{\%_{N2,out}} \quad (4)$$

Flow of product A:
$$F_A = F_{tot,out} * \%_{A,out} \quad (5)$$

3.2.4 Long-term performance tests

Long-term tests were used to evaluate the catalyst stability by measuring the increase in CH_4 concentration in the reactor effluent (i.e. the decrease in conversion) over a period of 100 h. The reaction was run at 600 °C which is within the expected operational temperature range of the fuel cell. Due to external circumstances, the GC was not available for the long-term tests, and instead the Gasmitter was used to measure the CH_4 effluent concentration. The conversion of CH_4 could then be calculated (see Calculations).

Calculations

Without the GC, the effluent N_2 concentration is unknown which means it cannot be used to calculate the total flow as was done for the activity tests. Instead, a mass balance of carbon is made. The ratios of CO/CO_2 and H_2/H_2O are unknown, but since only CH_4 conversion is interesting for the long-term tests, these can be lumped together into one term each. For each mole of reacted CH_4, one mole of CO/CO_2 will be formed, and two moles of H_2/H_2O will be formed, leading to the mass balance shown in 7.2. The conversion of CH_4 (eq. 6) can be calculated from the detected outlet CH_4 concentration according to the equation below. For the complete calculation, see 7.2.

Conversion of methane:
$$x = 1 - \frac{6.5 * \%_{CH4}}{1 + 2 * \%_{CH4}} \quad (6)$$

With $\%_{CH4}$ being the outlet concentration of CH_4.

3.3 Characterization

After the testing phase, characterization was performed on β-C1, β-CS4, C1 and CS4 at the LTH Chemical Centre in Lund using a Micromeritics 3Flex BET/Chemisorption analyzer. The 3Flex is equipped with a gas injection system, a furnace and a TCD. For each test, a sample of around 1 g of catalyst particles was placed into a quartz tube and supported at both ends by glass wool. The effluent gas was cooled by a cold trap using isopropanol chilled with liquid nitrogen.

3.3.1 TPR

Temperature-programmed reduction with 10% H_2 in Ar was performed on β-C1 at 50-700 °C and 1 atm. The temperature ramp was 10 °C/min, with one measurement every 0.10 s.

3.3.2 Chemisorption

Dynamic CO chemisorption was performed on fresh β-C1, β-CS4, C1, CS4, and spent β-C1 and β-CS4. The samples were reduced with 10% H_2 in Ar at 400 °C for 60 min, after which cooling to 35 °C and purging with He took place. 0.5 ml of CO was then dosed repeatedly until complete saturation. Finally, the samples were purged for 5 min with N_2. Catalyst active phase surface area, dispersion and average particle diameter were calculated using the 3Flex software. Static chemisorption experiments were also attempted but were unsuccessful due to equipment failure.

4 Results and discussion

The short-term activity tests show that all the 1% Ru and 2% Ru catalysts are active for the CPOM reaction, achieving conversion and product selectivity close to equilibrium. The long-term stability results on 0.5% Ru with and without addition of Mg (β-C1 vs β-CS4) show that the Mg significantly increases stability, although both catalysts continue to gradually deactivate even after 100h of reaction. A kinetic model is presented which predicts an almost double half-life for β-CS4 compared to β-C1.

4.1 Activity tests

Activity tests on C1, CA1, CA2, CA3, CA6 and CS4 were carried out, examining the CH_4 conversion and selectivity towards syngas. Figure 4.1 shows the methane conversion by the reference catalyst C1 at GHSV= 10,000 h^{-1}, with the theoretical equilibrium curve and a measurement with only inert material as comparison. For this catalyst, conversion reached around 90% of the equilibrium conversion, except for the point at 650 C which reached 99%. Comparing with the results for the inert material, it is evident that the catalyst is active, significantly increasing methane conversion. The product selectivity also shifts from mainly CO_2 and water to mainly syngas (Figure 4.2), approaching a favorable H_2/CO ratio of about 2 with increasing temperature. Unexpectedly, the conversion of methane is not zero for the experiment with only inert material, possibly due to residual contamination from previous experiments. It is also possible that the dry and steam reforming reactions can occur thermally at high temperatures (although not to the same extent as the catalyzed reaction) by contact with the reactor wall. This would explain the somewhat high selectivity towards H_2 at T>650 °C for the inert experiment. Nevertheless, from these experiments, the catalyst is clearly active and selective towards the desired products.

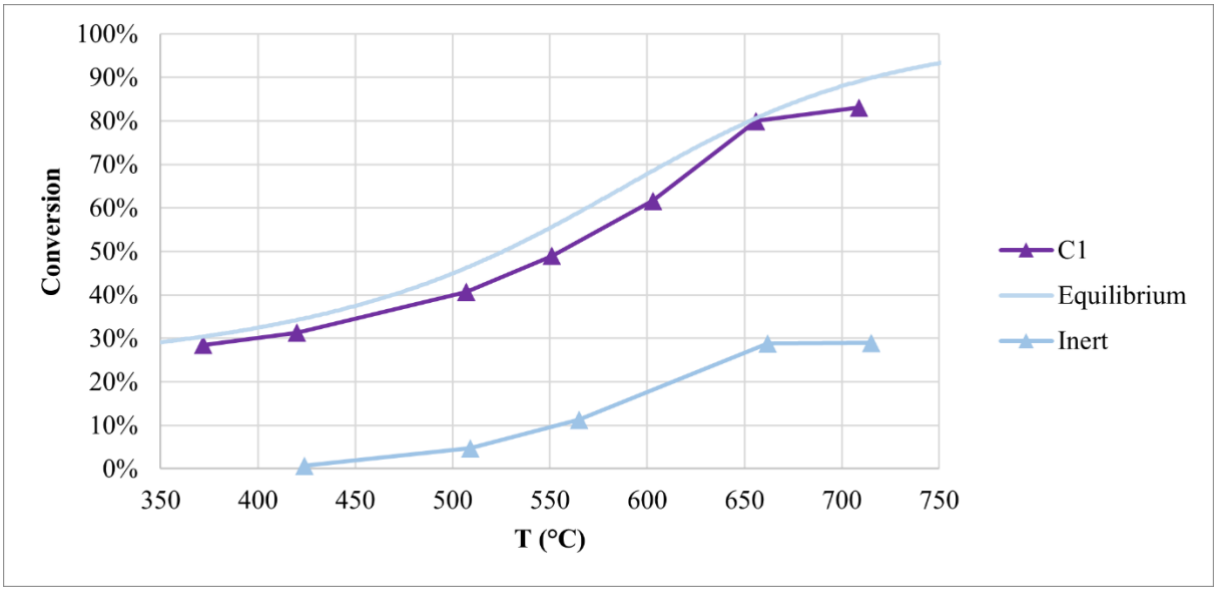

Figure 4.1: CH4 conversion for C1 at GHSV = 10,000 h^{-1} compared to inert material (alumina support) and equilibrium.

The CO and H_2 selectivity of C1 also follows the expected behaviour, as shown in Figure 4.2, with both selectivities mirroring near exactly the equilibrium selectivities predicted by the simulation. Thermodynamically, the formation of CO is favored at high temperatures since the

water-gas shift, dry reforming and steam reforming reactions (R3-R5) are endothermic. At lower temperatures, only total oxidation seems to occur, as expected. The formation of some H_2 at low temperatures is likely due to water-gas shift (R5), as this is an exothermic reaction with H_2 as the product. If any CO were formed, this reaction would shift most of it into CO_2, which is also consistent with the results.

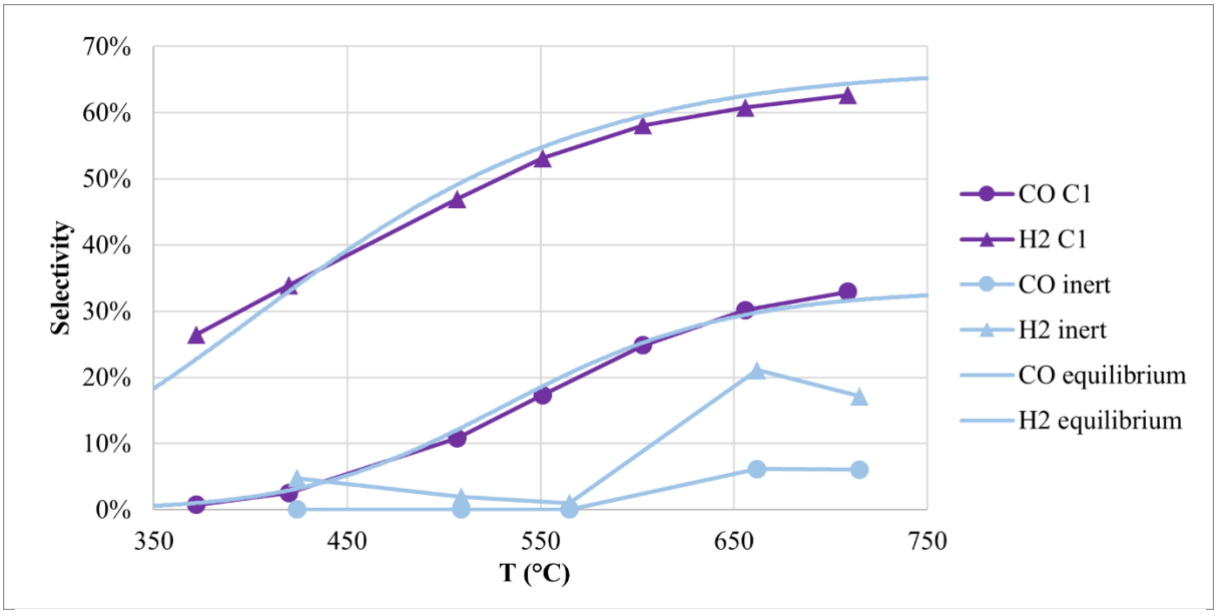

Figure 4.2: CO and H2 selectivity for C1 at GHSV = 10,000 h^{-1} compared to inert material and equilibrium.

The activity tests at GHSV = 10,000 h^{-1} were repeated for CA1, CA2, CA3, CA6 (i.e. the catalysts with modifications to the active phase), as well as for CS4 (10% added Mg). As shown in

Table 4.1 and Table 4.2, these tests all gave identical results as those of C1. At first it was suspected that some error in the method, such as reactor conditions or equilibration wait time was the explanation, but these were disproven. The inert test shows that different results are obtained when a catalyst is not present, and previous equilibration tests (performing a second GC measurement 30 min after the first one) shows that the equilibrium time and the time for the product gas to travel from the reactor to the analysis equipment is short. The results are also similar to those of Yan et al.[17] who performed activity tests on a 1% Ru catalyst under similar conditions. Instead, a more likely explanation is that all the catalysts are maximally active and are limited by mass transport rather than catalyst activity. When the reactants reach the catalyst surface, there seems to be enough active phase area in all catalysts to enable complete conversion at the investigated GHSV, and lowering the GHSV further would bring the reaction even closer to equilibrium. The first round of testing was therefore unable to show any significant difference between the catalysts, but show that even 1% Ru is enough to fully catalyze the reaction. The standard recipe could therefore be amended, as lowering the active phase content would have no negative impact on activity but would reduce catalyst cost. However, comparative long-term tests on the 2% and 1% catalysts would be required to verify that the stability is also unaffected before making this decision.

Table 4.1. CH_4 conversion at GHSV = 10,000 h^{-1}.

	500 °C	**550 °C**	**600 °C**	**650 °C**	**700 °C**
Equilibrium (%)	44.9	55.4	67.8	79.4	88.0
C1 (%)	40.7	49.0	66.5	79.0	83.1
CA1 (%)	43.5	-	62.1	-	83.9
CA2 (%)	42.4	-	62.3	-	83.5
CA3 (%)	-	-	61.6	-	83.7
CA6 (%)	-	-	62.0	-	84.1
CS4 (%)	39.7	-	66.9	74.3	83.3

Table 4.2. Product selectivities at GHSV = 10,000 h^{-1}.

	500 °C		**550 °C**		**600 °C**		**650 °C**		**700 °C**	
	CO	**H_2**	**CO**	**H_2**	**CO**	**H_2**	**CO**	**H_2**	**CO**	**H_2**
Equilibrium (%)	11.1	48.1	18.5	54.7	24.9	59.3	29.1	62.3	31.3	64.0
C1 (%)	10.8	46.9	17.3	53.1	24.8	58.1	30.1	60.8	32.9	62.7
CA1 (%)	10.5	48.3	-	-	25.1	57.8	-	-	32.7	62.7
CA2 (%)	10.0	48.8	-	-	25.4	57.9	-	-	33.0	62.8
CA3 (%)	-	-	-	-	25.1	57.8	-	-	32.1	63.3
CA6 (%)	-	-	-	-	25.1	58.2	-	-	32.2	63.4
CS4 (%)	9.9	46.1	-	-	25.1	57.7	30.1	60.9	32.7	62.9

4.1.1 Changing reactor conditions

The results from the activity tests suggested that mass transfer limitations are affecting the reaction; reactants react immediately upon reaching the surface due to a surplus of available active phase. The occurrence of mass transfer limitation can be shown by varying GHSV as this reduces residence time and therefore allows more active sites to be utilized. Increasing the GHSV should cause the selectivity to change as the secondary reactions should not be able to occur to the same extent. A decrease of conversion should also occur as less of the methane should have time to reach the catalyst surface. For this reason, tests were conducted on C1, varying the GHSV from 10,000 to 160,000 h^{-1}, which was the maximum possible GHSV for the equipment. However, the results of these tests were also very similar to the standard case. The conclusion drawn from this is that the catalyst is indeed very active, as not even at 16 times the standard GHSV, a decrease of the conversion was seen. To be able to see a difference, a second batch of catalysts with lowered active phase content (the β-series) was prepared, which contained 0.5 % Ru and 0.125 % promotor metal in the applicable cases. The β-series was then investigated in the long-term tests.

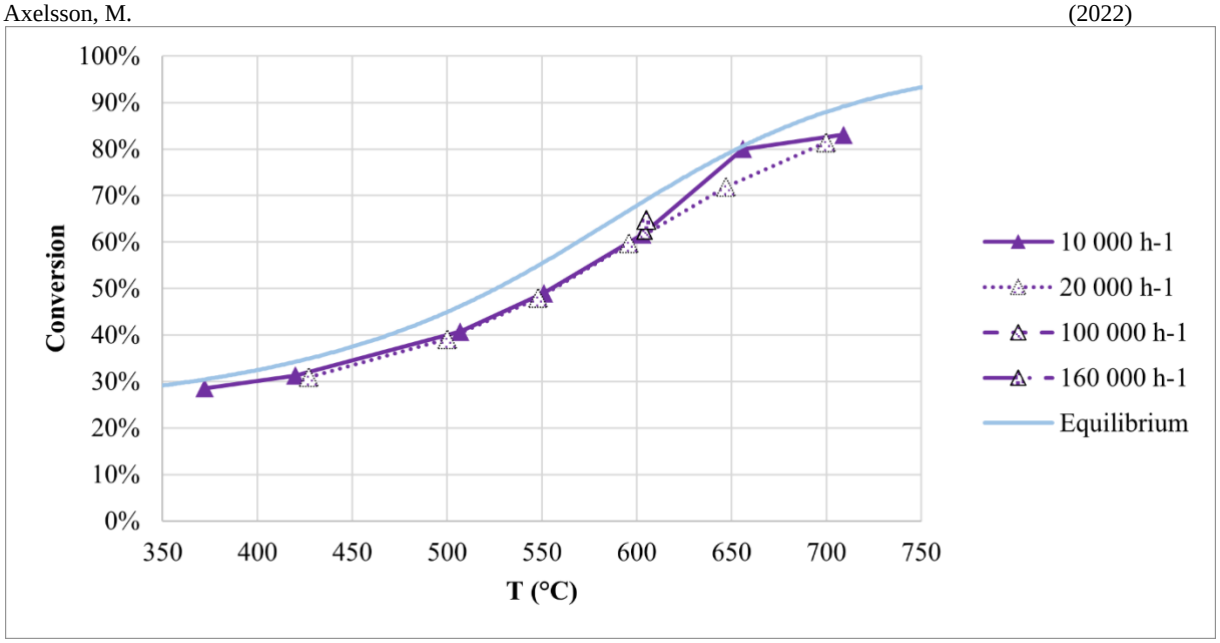

Figure 4.3: Effect of GHSV increase on C1.

Additionally, some changes to the reactor bed were investigated. In the previous tests, the size of the inert particles was larger than the catalyst particles to allow for separation of the catalyst particles after the reaction. However, the large grain size possibly enables channel formation in the catalyst bed, allowing reactants to pass through without interacting with the bed and thus lowering activity. The difference in size is necessary for sieving the inert from the catalyst in preparation for analysis, but having the inert particles be smaller rather than larger might reduce the channel formation. A test with smaller particles was carried out at 100,000 h^{-1} (Table 4.3) which showed an increase in conversion compared to the same GHSV with larger particles, supporting the idea that channel formation occurred in the first tests. However, this does not change the other conclusions drawn, as the effect of changing the inert size on the catalyst activity would be the same for all catalysts, and thus a difference between the previously discussed catalysts would still not be observable.

The second change was the lowering of the height of the catalyst bed, which could reduce the activity of the catalyst. A long bed increases the risk of thermal and concentration gradient formation. For example, in a long bed, the influx of oxygen might cause the volatilization of Ru. If gradients are present, as the Ru travels down the bed, the more reduced atmosphere further down the bed could cause the Ru to be re-reduced onto the surface. The longer the bed is, the more times this can happen before the activity is reduced. As most of the deactivation happens early, this effect could affect the results of the activity tests. To investigate, a test was carried out with a halved amount of inert and catalyst (total 11 ml instead of 22 ml), reducing the flow rate to maintain the same GHSV. The result is shown in Table 4.3: the halved bed length indeed reduces conversion. Worth mentioning is that due to external circumstances, the gasmitter was used instead of the GC for this measurement, meaning that the result is not quantitatively comparable to the one made with the GC, as the precision of the gasmitter is lower. However qualitatively the conclusion can be drawn that the conversion of methane is lower for the smaller bed compared to the large one, supporting the hypothesis of volatilization followed by reduction. As this suggests the presence of gradients in the system, it becomes even more important to investigate the catalysts with lower active phase content. Again

however, the results of the previously tested catalysts remain valid as the gradient effect should be the same in all cases.

Table 4.3: CH_4 conversion at 600 °C and GHSV = 100,000 h^{-1} when altering the inert particle size and bed length.

	Large inert particles	**Small inert particles**	**Small inert particles + halved bed length**
CH_4 conversion	62.2%	66.8%	52%

4.2 Long-term performance tests

High catalyst activity does not guarantee that the catalyst will also be stable. It is possible that a catalyst will be highly active in the beginning, then rapidly deactivate, in which case it will not be useful in most commercial applications. For this reason, it is important to examine the long-term catalytic behavior as well.

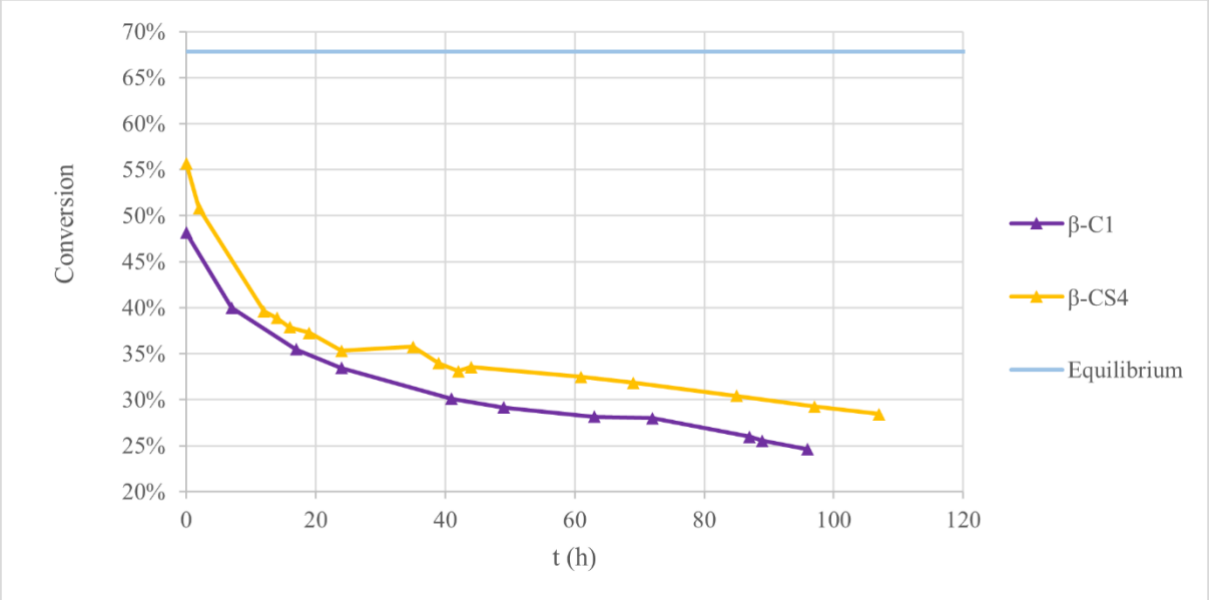

Figure 4.4: Long-term stability tests for β-C1 (0.5% Ru) and β-CS4 (0.5% Ru with 10% added Mg).

Long-term tests were carried out for 100 h at GHSV = 50,000 h^{-1} and 600C for β-C1 and β-CS4. Figure 4.4 shows the deactivation processes for these catalysts. β-C1 shows a rapid exponential decrease in CH_4 conversion for the first 20 hours, followed by a sustained linear decrease for the rest of the 96h measurement period. The deactivation is both rapid and significant with conversion reduced from 49% at t=0h to 25% at t=96h, with no stabilization during the time frame. As the conversion depends on the GHSV and operational temperature of the fuel cell, which may be different than the conditions in the experiment, the absolute value of the deactivation is less interesting than the relative decrease in conversion. As the long-term tested catalysts only had 0.5% Ru instead of 1-2% as during the activity tests, it is likely that the threshold where lowered activity starts was reached. This explains why the long-term tested catalysts have lower initial activity than the 2% catalysts had at the same temperature during the activity testing. The catalyst loading in the application would have to be compensated for to ensure activity for the required 100 hours though, leading to higher costs if deactivation is

high. Compared to the results of Velasco et al.[4], which saw a slower deactivation for their 1% Ru/alumina catalyst, this deactivation is much faster. This is reasonable, however, since the conditions in this experiment are harsher: the GHSV is lower and the CH_4 and O_2 content in the inlet gas is higher. At these conditions, the likelihood of sintering due to hot spot formation is higher which would result in a more rapid deactivation.

β-CS4 shows a smaller total decrease in conversion than β-C1, with a final conversion of 30% after 100 h. Notably, the initial activity of β-CS4 is much higher than that of β-C1. As the two catalysts have the same active phase, their initial conversion should be the same. The likely reason for this is that the time 0h is actually different for the two catalysts. The time is measured from the point where the reaction has stabilized at 600 °C, which may vary depending on the practical circumstances of the experiment. During this start-up phase, some deactivation will occur, affecting the "initial" conversion value. Additionally, if there is a stabilizing effect of the addition of Mg, which the results suggest, the deactivation taking place during the heating and equilibration phase would likely also be less extensive for β-CS4 than for β-C1. These factors, on their own or taken together, can explain why the initial conversion differs between the catalysts. Possibly, the extra Mg could also be catalytically active; this can unfortunately not be disproven by the activity tests since the activity was maximal for both C1 and CS4.

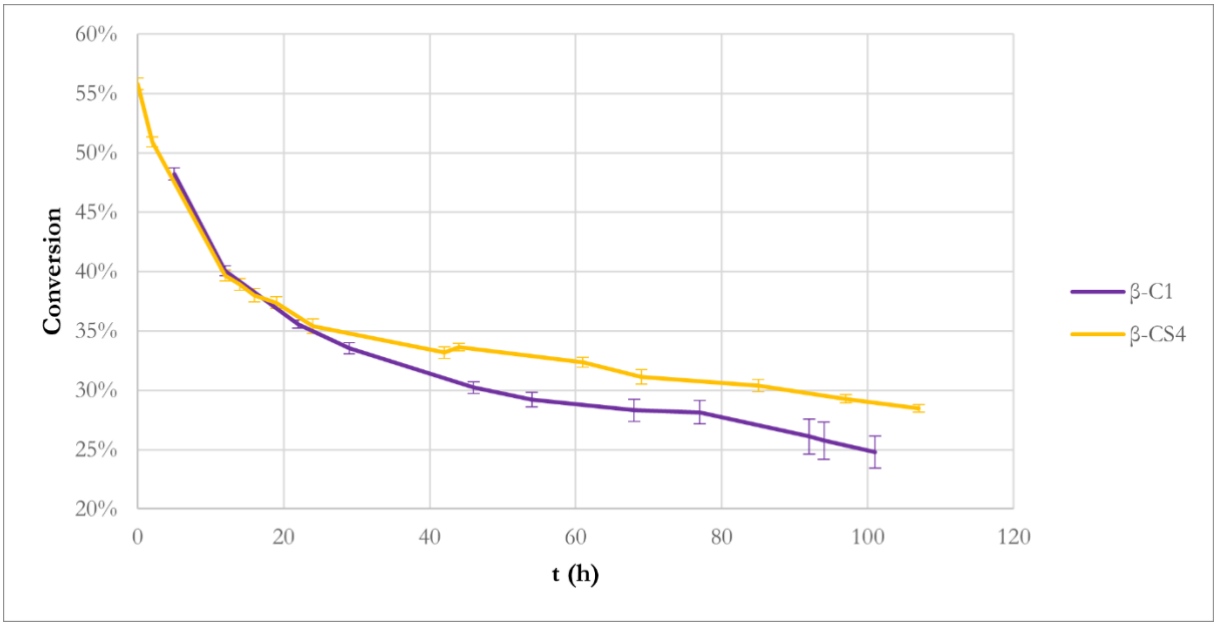

Figure 4.5: Time zero-adjusted long-term tests for β-C1 and β-CS4.

To compensate for the difference, Figure 4.5 shows the results for β-C1 with a time adjustment which gives the two samples the same initial activity (calculated using the kinetic model introduced later in the report), which showcases the differences more representatively. The effect on stability is evident, with β-CS4 deactivating more slowly than β-C1, although neither is completely stable after 100 h. Interestingly, the initial deactivation occurs at the same rate for both catalysts, but the subsequent linear deactivation rates are different, with CS4 deactivating more slowly and therefore achieving a higher final conversion. As the deactivation process is complex with multiple sub-processes (sintering, coking) occurring simultaneously, it is possible that the linear regime is dominated by a different type of deactivation compared to the exponential regime, and that the addition of magnesium limits this type of deactivation. Specifically, as magnesium is thought to reduce the number of acid seats on the catalyst surface,

deactivation due to coking may have been less extensive in β-CS4 than in β-C1, resulting in an overall increase in long-term stability. It is also reasonable for the rate of sintering to be higher early in the deactivation process, as the clustering of active phase particles would be favored by a high degree of dispersion. However, as shown later by chemisorption experiments, the initial degree of dispersion of β-CS4 is higher than that of β-C1, meaning that the initial deactivation rate should be higher for β-CS4.

For β-CS4, around t = 40h, the conversion temporarily increases before continuing to decline, likely due to measurement error in the previous point. This is further examined in the *Data reliability* section of the report.

Overall, the long-term test results show that the addition of 10% Mg to the formulation improves catalyst stability, although a linear decline in conversion is observed even after 100 hours. For commercial viability, the stability likely needs to be improved further, as the cost of ruthenium will be difficult to justify if the catalyst loading needs to be very large to compensate for deactivation.

4.3 Data reliability

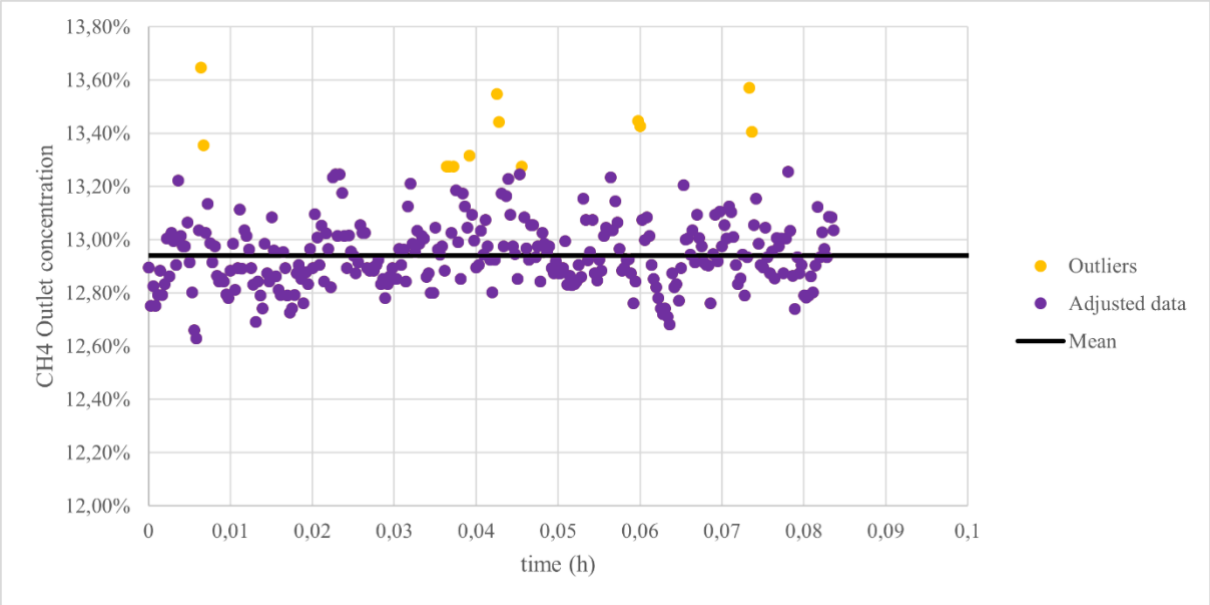

Figure 4.6: Typical distribution of measurement data (taken from t=42h, β-CS4).

During the long-term testing, some strange behavior was observed, warranting further inspection. In the long-term tests, the concentration of CH_4 in the outstream was continuously registered by the detector with an interval of 3 seconds. The data collection was performed by sampling data points over a 15 min period and using the average value as the result. This was done because measurement noise is quite high due to the high sampling frequency and the detector accuracy of ±0.2 %. Outliers outside of the mean value ±1.5 standard deviations were trimmed to increase accuracy. A typical result is shown in Figure 4.6 with data points distributed evenly over the mean value. Nevertheless, some inconsistencies were found, namely:

1. For β-CS4, the conversion suddenly increased around t=40h after which it continues to decrease.
2. For β-C1, the margin of error increased over time.

Most data samples resemble Figure 4.6, with an even data distribution. At t=35h and t=39h for β-CS4, however, the spread of the data deviates from the expected behavior, as shown in Figure 4.7. The data distribution suddenly narrows, leading to an underestimation of the CH_4 outlet concentration. This temporary anomaly was only observed in these points, and a reasonable explanation has not been found. Giving the mean value of these two measurements would not be representative, and they were therefore discarded.

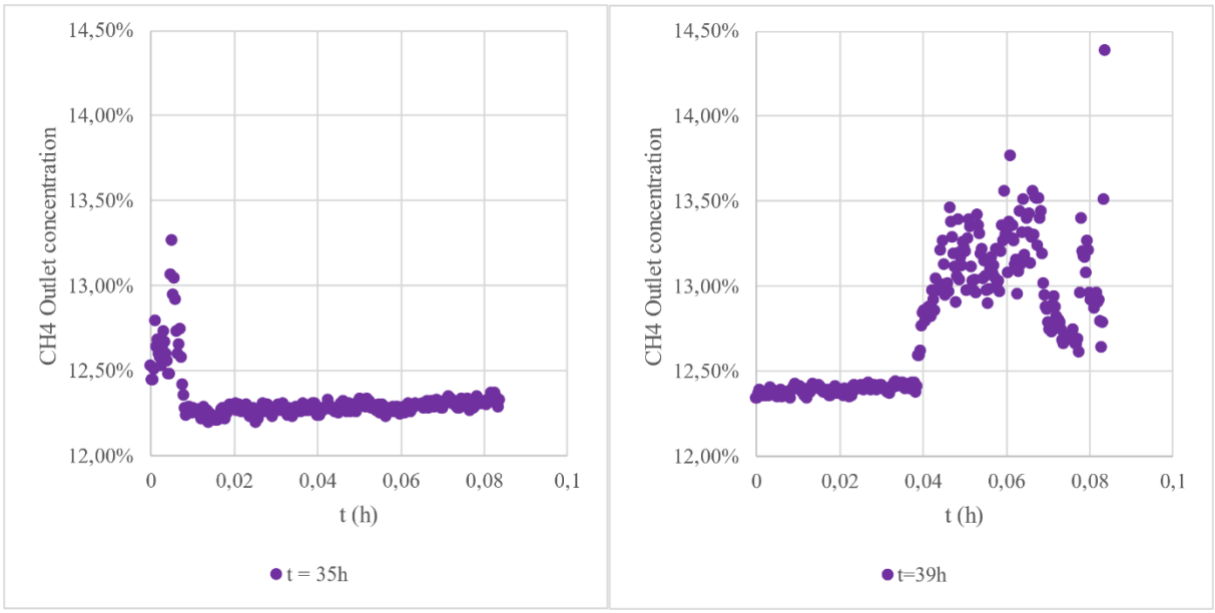

Figure 4.7: Data anomalies observed at t=35h and t=39h for β-CS4.

Additionally, an increase in data variance with time (heteroscedasticity) was observed for β-CS4, but not for β-C1, even after adjusting for outliers. A proposed explanation for this was the accumulation of water in the collection vessel. During the reaction, some water will form, and in case the vessel is not emptied, some of the water can be swept with the gas into the analysis equipment, distorting the results by increasing the noise. However, the vessel was emptied halfway through the process for both β-C1 and β-CS4, and the amount of water was not very large, filling less than half of the vessel.

4.4 Kinetic modeling of deactivation

To further explain the shape of the deactivation curve for the long-term tests, and to predict the half-life of each catalyst, a kinetic model was developed, based on the work of Brandin and Odenbrand (2018)[18]. If the deactivation is seen as a decrease in reaction rate over time, an expression for the conversion x as a function of time can be calculated. In Brandin and Odenbrand's model, the preexponential factor is a function of ln(1-x) and a number of constant reaction parameters. Using this as a basis for the development and assuming a 1st order reaction with respect to CH_4, the expression for the conversion becomes:

$$x(t) = 1 - e^{(Ae^{Bt+C})} \qquad \textit{(Model 1)}$$

Where A, B and C are constants. A is related to the physical parameters of the model and B and C are fitting constants. A full derivation of the expression can be found in 7.3. Through iterative fitting of the parameters for each set of experimental data, the model fit shown in Figure 4.8 is obtained. The model (*Model 1*) follows the experimental data quite well during the rapid deactivation part and has an overall R^2 value of 0,95 and 0,97 for β-C1 and β-CS4, respectively. However, the model levels out at high t and thus does not account for the linear part of the deactivation process.

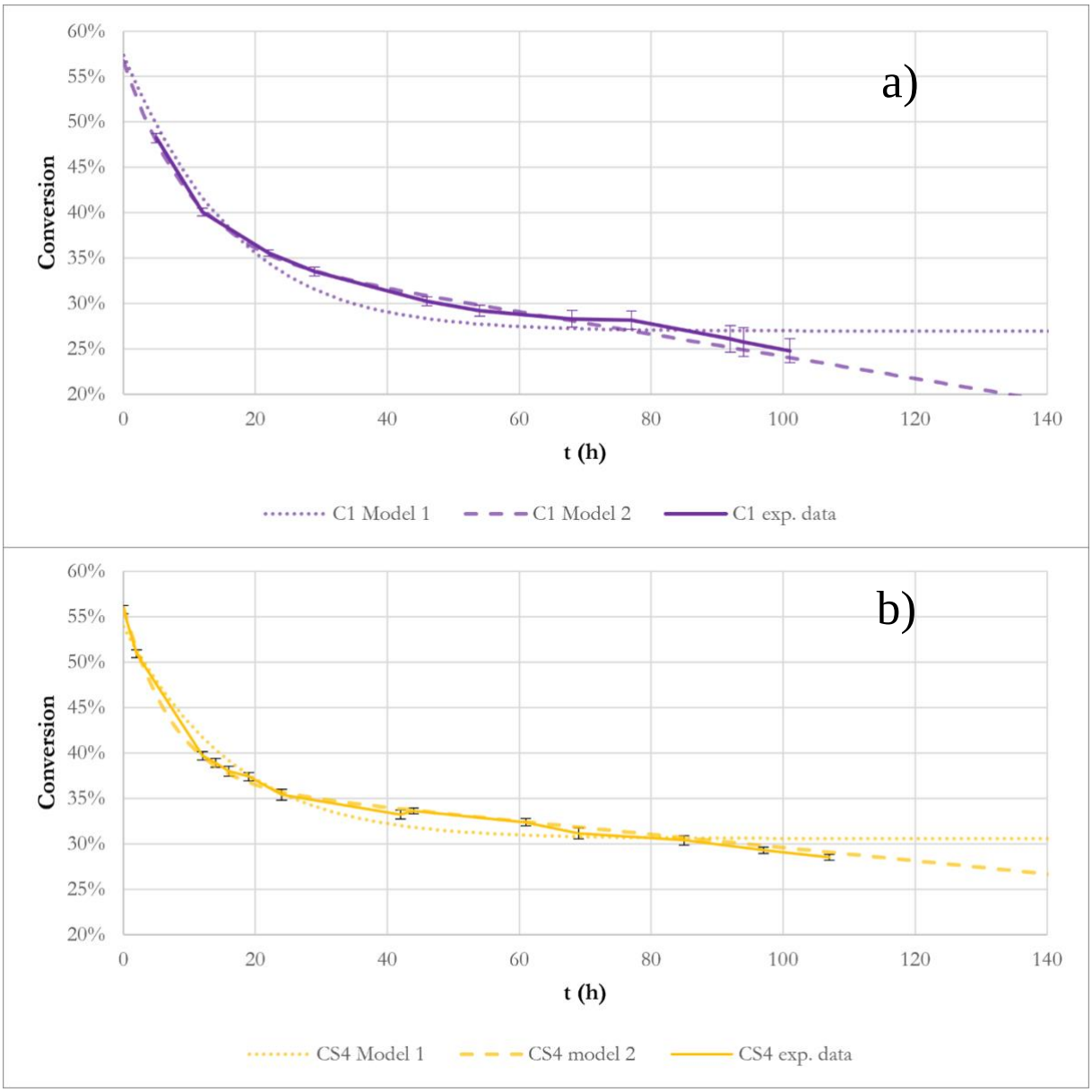

Figure 4.8. CH4 conversion models for a) β-C1 and b) β-CS4.

To be able to calculate the half-life of the catalysts (the time for the catalyst to deactivate to 50% of the initial conversion, adjusted for t=0), the model was complemented with a linear decrease based on the slope of the linear part of the curve, making the model (Model 2):

$$x(t) = 1 - e^{(Ae^{Bt+C})} + x'_{exp} * t \qquad \textit{(Model 2)}$$

Where x'_{exp} is the average slope of the linear portion of the curve for each catalyst. At high t, model 2 becomes a simple linear equation and thus has no physical backing. This brings the model onto "thin ice" since it is not certain that the catalyst will continue to deactivate at the same rate in the long turn. The half-life obtained through Model 2 should therefore be interpreted only as an indicator of catalyst stability and not necessarily as a real half-life. It does however take into account the non-linear behavior exhibited early in the deactivation process. With this reservation in mind, the half-life of β-C1 was determined[1] to be 69h, and for β-CS4 123h, which gives an indication of the difference in catalyst amount that would be required to compensate for loss in activity. The addition of the linear term also improves the fit for the non-linear part of the curve, suggesting that the mechanism causing the linear decrease operates in tandem with the mechanisms predicted by Model 1.

β-CS4 thus appears significantly more stable than β-C1, however more improvements need to be made to stabilize it further, for example by testing the catalyst modifications which were not able to be tested during this project.

4.5 Characterization results

Dynamic (pulse) chemisorption was performed on fresh and long-term tested β-C1 and β-CS4, resulting in values for metal surface area, metal dispersion and average particle diameter. Analysis of fresh C1 and CS4 (i.e., with 2% Ru) were also tested for reference. The results show that fresh β-CS4 has higher surface area than fresh β-C1, attributed to higher stability during calcination.

4.5.1 Pulse chemisorption

The surface properties of the long-term tested catalysts from the dynamic CO chemisorption are shown in Table 4.4. Fresh β-CS4 has a larger total active phase surface area than β-C1, at 0.21 m^2/g and 0.14 m^2/g, respectively. This suggests that the addition of Mg during the formulation phase increases stability during calcination, and can also explain the higher initial activity of β-CS4 during the long-term testing. Compared to the Ru/Al_2O_3 catalyst prepared by Velasco et al.[4], which had a surface area of 0.2 m^2/g with 1% Ru, this result seems reasonable as the degree of dispersion of β-C1 and β-CS4 is about double with half the particle diameter.

Interestingly, the results for the spent catalyst samples do not show a loss of surface area, as would be expected after 100 hours of testing. β-CS4 even has a significantly larger surface area after testing than before. A possible, though unlikely explanation is that Ru impregnated in the support pores has migrated onto the outer surface by volatilization. However, this should also mean that the long-term tests should not have shown such an extensive decay, but rather the conversion should have been maintained. The same can be said for β-C1; if the surface area was slightly higher after 100 hours, this should have been reflected in the stability tests. A more likely explanation for the results is the measurement uncertainty of the sample, which mainly stems from two factors. First, the sample heterogeneity for the spent catalysts. After the testing, the inert material was sieved away, however some particles close in size to the catalysts remained in the sample and were included in the weight of the sample upon characterization. This results in an underestimation of the actual surface area, however, and so does not explain why the surface area is higher for the spent catalyst. Rather, the reason is probably that the amount of material used is insufficient. During the testing, only 2 ml of catalyst was used, meaning only around 0.5 g of catalyst grains were available for analysis afterwards. As the

[1] This value is within the experimental data and can of course be determined without the model as well.

pulse volume was 0.5 ml of pure CO (no diluted CO was available, unfortunately), and the loading of Ru was only 0.5%, the pores were almost completely filled after the first pulse, meaning the difference between the first and second pulse was very small, resulting in high measurement uncertainty. The spent samples could be remeasured by removing the chemisorbed CO through temperature programmed desorption (TPD), however this was not attempted due to lack of time.

Table 4.4. Results from dynamic CO chemisorption.

	β-C1 (fresh)	**β-CS4 (fresh)**	**β-C1 (spent)**	**β-CS4 (spent)**	**C1 (fresh)**	**CS4 (fresh)**	**Velasco et al.**[4] **(1% Ru/Al2O3)**
Cumulative quantity (cm3/g STP)	0.08	0.11	0.09	0.20	0.62	0.33	-
Metal dispersion	7.1%	10.3%	7.7%	18.2%	14.1%	7.4%	*4.1%*
Metallic surface area (m^2/g sample)	0.14	0.21	0.16	0.37	1,14	0.60	*0.2*
Metallic surface area (m^2/g metal)	29	42	31	73	57	30	-
Active particle diameter (hemisphere) (Å)	170	116	156	66	85	162	*310*
Cubic crystallite size (Å)	141	97	130	55	71	135	-

Furthermore, the CO chemisorption results for the 2% Ru catalyst are also interesting. CS4 has 3x the surface area of β-CS4, which is expected considering the 4x higher metal loading and reduced surface area due to clustering (more clustering with high loading). Repeated tests on C1, however, resulted in 10x the surface area of β-C1, with a much higher degree of dispersion. An explanation for this in the formulation and pretreatment could not be found as C1 was prepared in the same way as CS4 and the β-catalysts. Unusually high presence of a higher level of catalyst particle dust in this sample (particles with low binder content being broken down during calcination and retrieval) is suggested as an explanation.

Lastly, H_2 pulse chemisorption was also performed on β-C1, resulting in almost no chemisorbed gas. This is most likely due to the slow adsorption equilibrium of Ru-H_2, as described by Okal et al.[16].

4.5.2 Temperature programmed reduction (TPR)

TPR was performed on β-C1, showing a large peak at around 160 °C (Figure 4.9). Comparing to literature results (Shi et al.[19]), the peak is attributable to the reduction of RuO_2 → Ru. This result means that the active phase is activated already at below 200 °C, meaning the pretreatment temperature could possibly be reduced which would lower metal particle clustering if desired. Since the catalyst is highly active, however, there is no need to increase the surface area. Instead, from a stability perspective, it might be preferable to maintain the high temperature for a longer time to induce more particle clustering, as larger particles will take longer to sinter, which would increase the lifetime of the catalyst.

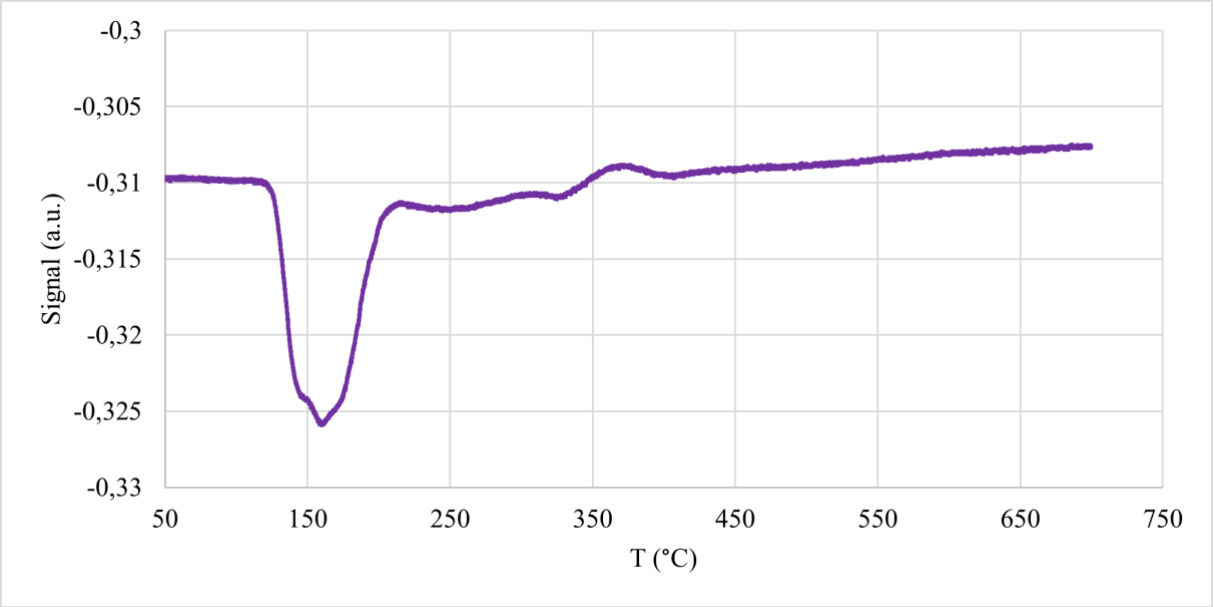

Figure 4.9. TPR performed on β-C1. Peak around 160 °C attributable to RuO_2-->Ru reduction.

5 Conclusion

In this work, 20 Ru-based catalysts were prepared by incipient wetness impregnation. Out of these, six catalysts with different active phase composition were tested for activity. Two catalysts were tested for long-term stability to investigate a modification to the support. The activity tests show that all catalysts give conversion of methane and selectivity towards syngas close to the thermodynamic equilibrium, with a H_2/CO ratio close to 2, even at low metal loading and high space velocity. The long-term tests show that the addition of 10 wt% magnesium to the support significantly increases the lifetime of the catalyst, although further improvements are needed to achieve satisfactory stability. Kinetic modelling of the stability tested catalyst deactivation gives a half-life of 123 h for the magnesium-doped catalyst, compared to 69 h for the non-doped. Catalysts doped with small amounts of platinum and palladium were also prepared and showed high activity, however these were not stability tested due to time constraints.

Pulse chemisorption of the stability tested catalysts showed increased metal dispersion and surface area for the magnesium-doped catalyst compared to the non-doped. This suggests that the addition of magnesium improves stability during the pretreatment steps, i.e., calcination and activation. The results for the spent catalysts were inconclusive due to the scarcity of tested particles.

The addition of magnesium proved beneficial for catalyst stability, and further long-term tests to optimize the content are advised. Three catalyst formulations (CS1-CS3) are available for this, and catalysts with >10% Mg could also be synthesized. Furthermore, activity tests on the active phase-modified β-series with even higher space velocities could verify that all catalysts give the same selectivity towards syngas. Subsequent long-term testing on these, particularly on β-CA3 (co-impregnated Pt) and β-CA6 (Pt impregnated in series) would be interesting for the potential anchoring effect of Pt. Finally, investigations on the Gasmitter detector anomalies observed during the long-term tests should be made to ensure that results are consistent.

6 References

(1) Ritchie, H.; Roser, M.; Rosado, P. Energy. *Our World Data* **2022**. https://ourworldindata.org/energy.

(2) Lanza, R.; Velasco, J. A.; Järås, S. G. Recent Developments and Achievements in Partial Oxidation of Methane with and without Addition of Steam. In *Catalysis*; Royal Society of Chemistry: Cambridge, 2011; Vol. 23, pp 50–95. https://doi.org/10.1039/9781849732772-00050.

(3) Lin, Y.; Zhan, Z.; Liu, J.; Barnett, S. Direct Operation of Solid Oxide Fuel Cells with Methane Fuel. *Solid State Ion.* **2005**, *176* (23–24), 1827–1835. https://doi.org/10.1016/j.ssi.2005.05.008.

(4) Velasco, J. A.; Fernandez, C.; Lopez, L.; Cabrera, S.; Boutonnet, M.; Järås, S. Catalytic Partial Oxidation of Methane over Nickel and Ruthenium Based Catalysts under Low O 2 /CH 4 Ratios and with Addition of Steam. *Fuel* **2015**, *153*, 192–201. https://doi.org/10.1016/j.fuel.2015.03.009.

(5) Goodman, E. D.; Latimer, A. A.; Yang, A.-C.; Wu, L.; Tahsini, N.; Abild-Pedersen, F.; Cargnello, M. Low-Temperature Methane Partial Oxidation to Syngas with Modular Nanocrystal Catalysts. *ACS Appl. Nano Mater.* **2018**, *1* (9), 5258–5267. https://doi.org/10.1021/acsanm.8b01256.

(6) Smith, M. W.; Shekhawat, D. Catalytic Partial Oxidation. In *Fuel Cells: Technologies for Fuel Processing*; Elsevier, 2011; pp 73–128. https://doi.org/10.1016/B978-0-444-53563-4.10005-7.

(7) Trading Economics. *Nickel*. tradingeconomics.com. https://tradingeconomics.com/commodity/nickel.

(8) Umicore Precious Metal Management. *Ruthenium price*. pmm.umicore.com. https://pmm.umicore.com/en/prices/ruthenium/.

(9) Lanza, R.; Järås, S. G.; Canu, P. Partial Oxidation of Methane over Supported Ruthenium Catalysts. *Appl. Catal. Gen.* **2007**, *325* (1), 57–67. https://doi.org/10.1016/j.apcata.2007.03.005.

(10) Ballarini, A.; Benito, P.; Fornasari, G.; Scelza, O.; Vaccari, A. Role of the Composition and Preparation Method in the Activity of Hydrotalcite-Derived Ru Catalysts in the Catalytic Partial Oxidation of Methane. *Int. J. Hydrog. Energy* **2013**, *38* (35), 15128–15139. https://doi.org/10.1016/j.ijhydene.2013.08.135.

(11) Maniecki, T. P.; Bawolak-Olczak, K.; Mierczyński, P.; Maniukiewicz, W.; Jóźwiak, W. K. Effect of the Chemical Composition of (MgO)x(Al2O3)y Support on the Catalytic Performance of Ni and Ni–Au Catalysts for the Partial Oxidation of Methane. *Chem. Eng. J.* **2009**, *154* (1–3), 142–148. https://doi.org/10.1016/j.cej.2009.05.007.

(12) Lanza, R.; Canu, P.; Järås, S. G. Partial Oxidation of Methane over Pt–Ru Bimetallic Catalyst for Syngas Production. *Appl. Catal. Gen.* **2008**, *348* (2), 221–228. https://doi.org/10.1016/j.apcata.2008.06.044.

(13) Harris, D. C.; Lucy, C. A. *Quantitative Chemical Analysis*, Ninth edition.; W.H. Freeman & Company: New York, 2016 [633-648].

(14) Harris, D. C.; Lucy, C. A. *Quantitative Chemical Analysis*, Ninth edition.; W.H. Freeman & Company: New York, 2016. [650]

(15) Fadoni, M.; Lucarelli, L. Temperature Programmed Desorption, Reduction, Oxidation and Flow Chemisorption for the Characterisation of Heterogeneous Catalysts. Theoretical Aspects, Instrumentation and Applications. In *Studies in Surface Science and Catalysis*; Elsevier, 1999; Vol. 120, pp 177–225. https://doi.org/10.1016/S0167-2991(99)80553-9.

(16) Okal, J.; Zawadzki, M.; Kępiński, L.; Krajczyk, L.; Tylus, W. The Use of Hydrogen Chemisorption for the Determination of Ru Dispersion in Ru/γ-Alumina Catalysts. *Appl. Catal. Gen.* **2007**, *319*, 202–209. https://doi.org/10.1016/j.apcata.2006.12.005.

(17) Yan, Q. Partial Oxidation of Methane to H2 and CO over Rh/SiO2 and Ru/SiO2 Catalysts. *J. Catal.* **2004**, *226* (2), 247–259. https://doi.org/10.1016/j.jcat.2004.05.028.

(18) Brandin, J. G. M.; Odenbrand, C. U. I. Deactivation and Characterization of SCR Catalysts Used in Municipal Waste Incineration Applications. *Catal. Lett.* **2018**, *148* (1), 312–327. https://doi.org/10.1007/s10562-017-2229-8.

(19) Shi, J.; Hui, F.; Yuan, J.; Yu, Q.; Mei, S.; Zhang, Q.; Li, J.; Wang, W.; Yang, J.; Lu, J. Ru-Ti Oxide Based Catalysts for HCl Oxidation: The Favorable Oxygen Species and Influence of Ce Additive. *Catalysts* **2019**, *9* (2), 108. https://doi.org/10.3390/catal9020108.

7 Appendices

7.1 Appendix A: List of prepared catalyst recipes

Many more catalyst recipes were prepared than were able to be tested, due to time constraints. A complete list is given here, should there arise a desire to test them in the future.

Table 7.1: Complete list of prepared catalyst formulations for future research.

	Name	Support material	Support calcination temperature (°C)	Added Mg	Active phase	Activity tested?	Long-term tested?	Characterized?
1	C1	MG30	850	0%	Ru (2%)	Yes	No	Yes
2	CK1	MG30	900	0%	Ru (2%)	No	No	No
3	CK2	MG30	950	0%	Ru (2%)	No	No	No
4	CS1	MG30	850	1%	Ru (2%)	No	No	No
5	CS2	MG30	850	4%	Ru (2%)	No	No	No
6	CS3	MG30	850	7%	Ru (2%)	No	No	No
7	CS4	MG30	850	10%	Ru (2%)	Yes	No	Yes
8	CS5	MG70	850	0%	Ru (2%)	No	No	No
9	CA1	MG30	850	0%	Ru (1%)	Yes	No	No
10	CA2	MG30	850	0%	Ru (2%), Pd (0.5%)	Yes	No	No
11	CA3	MG30	850	0%	Ru (2%), Pt (0.5%)	Yes	No	No
12	CA4	MG30	850	0%	Ru (1%), Pd (0.5%)	No	No	No
13	CA5	MG30	850	0%	Ru (1%), Pt (0.5%)	No	No	No
14	CA6	MG30	850	0%	Ru (2%), Pt (0.5%), impregnated in series	Yes	No	No
15	β-C1	MG30	850	0%	Ru (0.5%)	No	Yes	Yes
16	β-CS2	MG30	850	4%	Ru (0.5%)	No	No	No
17	β-CS4	MG30	850	10%	Ru (0.5%)	No	Yes	Yes
18	β-CA2	MG30	850	0%	Ru (0.5%), Pd (0.125%)	No	No	No
19	β-CA3	MG30	850	0%	Ru (0.5%), Pt (0.125%)	No	No	No
20	β-CA6	MG30	850	0%	Ru (0.5%), Pt (0.125%), impregnated in series	No	No	No

7.2 Appendix B: Conversion calculation for long-term tests

The derivation of eq. 6 is given here. Table 7.2 shows the material balance for the reaction with inlet concentrations of 20% CH_4, 10% O_2 and 70% N_2. The material balance is used to calculate the methane conversion from the measured concentration of CH_4. F_{in} is the total flow of reactants, and $F_{CH4,out}$ is the outlet flow of CH_4. For every reacted CH_4 molecule, one molecule of CO/CO_2 and two molecules of H_2/H_2O are formed.

Table 7.2: Material balance for the reaction system.

	IN	**OUT**
CH_4	$0.2F_{in}$	$F_{CH4,out}$
O_2	$0.1F_{in}$	0
N_2	$0.7F_{in}$	$0.7F_{in}$
$CO+CO_2$	0	$0.2F_{in} - F_{CH4,out}$
H_2+H_2O	0	$2 * (0.2F_{in} - F_{CH4,out})$
Sum	$\boldsymbol{F_{in}}$	$\boldsymbol{1.3F_{in} - 2F_{CH4,out}}$

The value obtained from the long-term tests is $\%_{CH4}$, the CH_4 content in the outlet stream. This can be expressed as the outlet flow of CH_4 $(F_{CH4,out})$ divided by the total flow, according to the mass balance. This gives

$$\%_{CH4} = \frac{F_{CH4,out}}{1.3F_{in} - 2F_{CH4,out}} \Rightarrow F_{CH4,out} = \frac{1.3F_{in} * \%_{CH4}}{1 + 2 * \%_{CH4}} \quad \text{(B1)}$$

The conversion of methane, x_{CH4}, is calculated using equation B2, i.e.

$$x_{CH4} = \frac{F_{CH4,in} - F_{CH4,out}}{F_{CH4,in}} = 1 - \frac{F_{CH4,out}}{F_{CH4,in}} \quad \text{(B2)}$$

As the inlet concentration of methane is 20%, the inlet flow of methane is

$$F_{CH4,in} = 0.2F_{CH4,in} \quad \text{(B3)}$$

Which, combined with equation B1, gives the conversion of methane as a function of the measured % of methane according to

$$x_{CH4} = 1 - \frac{\frac{1.3F_{in} * \%_{CH4}}{1 + 2 * \%_{CH4}}}{F_{CH4,in}} = 1 - \frac{1.3F_{in} * \%_{CH4}}{F_{CH4,in} * (1 + 2 * \%_{CH4})} = 1 - \frac{1.3F_{in} * \%_{CH4}}{0.2F_{in} * (1 + 2 * \%_{CH4})}$$
$$= 1 - \frac{6.5 * \%_{CH4}}{1 + 2 * \%_{CH4}}$$

I.e. the equation used in the method section.

7.3 Appendix C: Derivation of kinetic model

The derivation of model 1 is shown below.

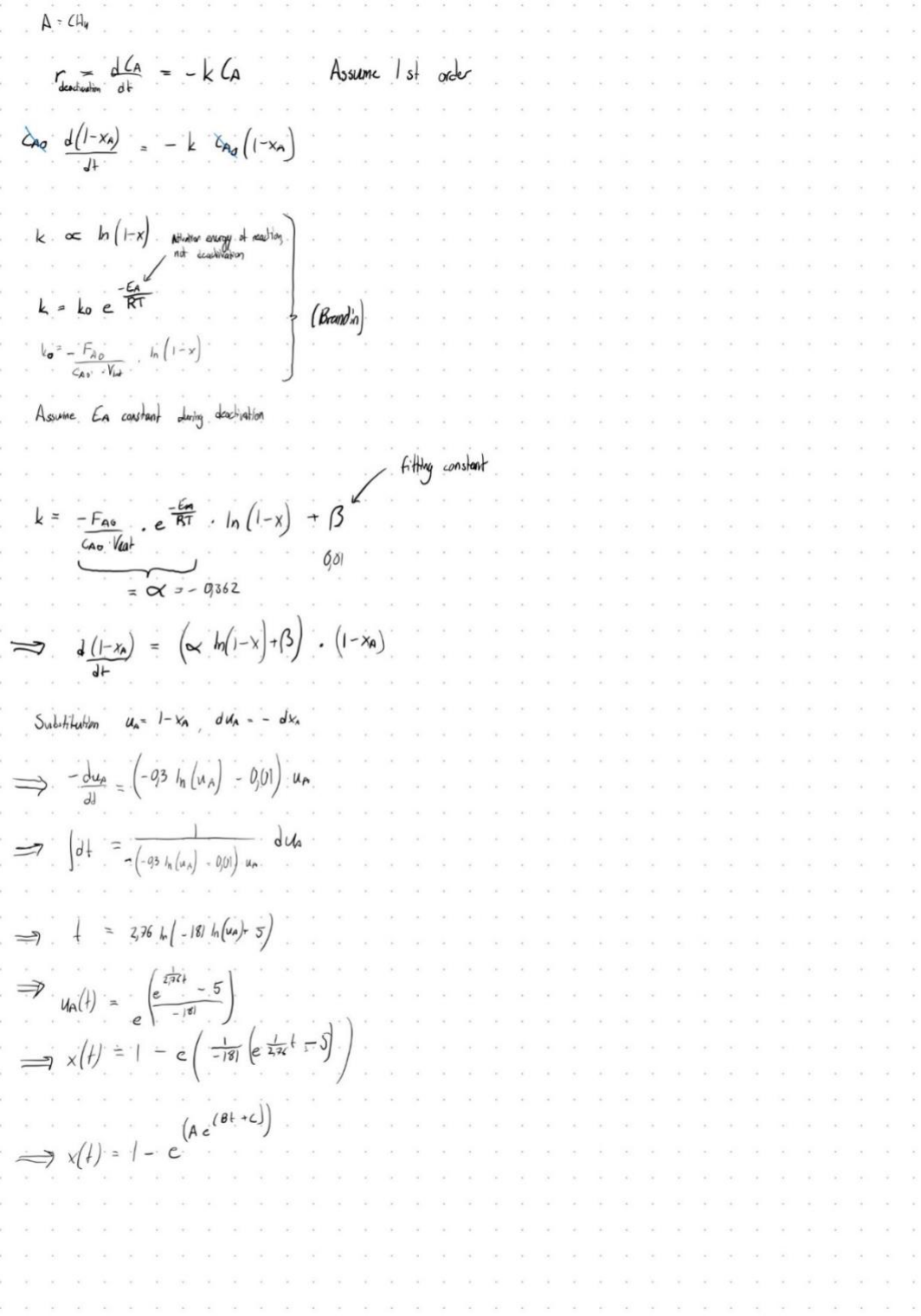

7.4 Appendix D: Supporting images

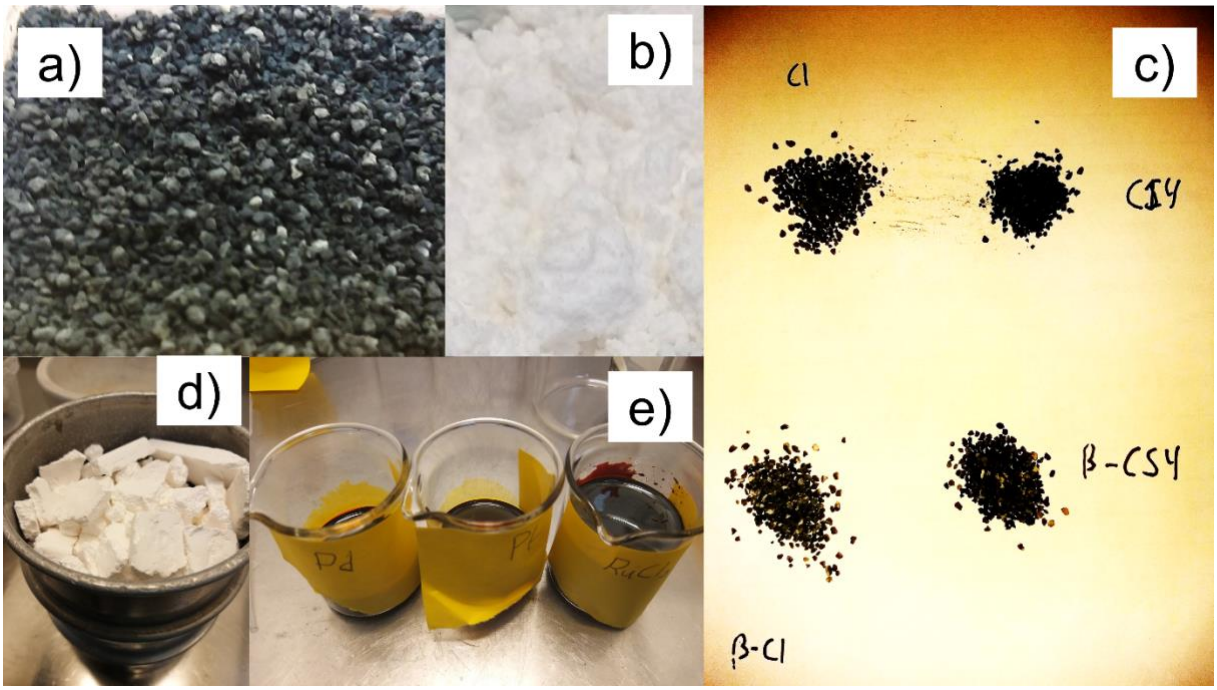

Figure 7.1. a) Ru-impregnated catalyst particles (C1). b) MG30 mixed with nyacol binder. c) Catalyst particles. d) Calcinated MG30+nyacol, to be mortared and sieved. e) Noble metal impregnation solutions.

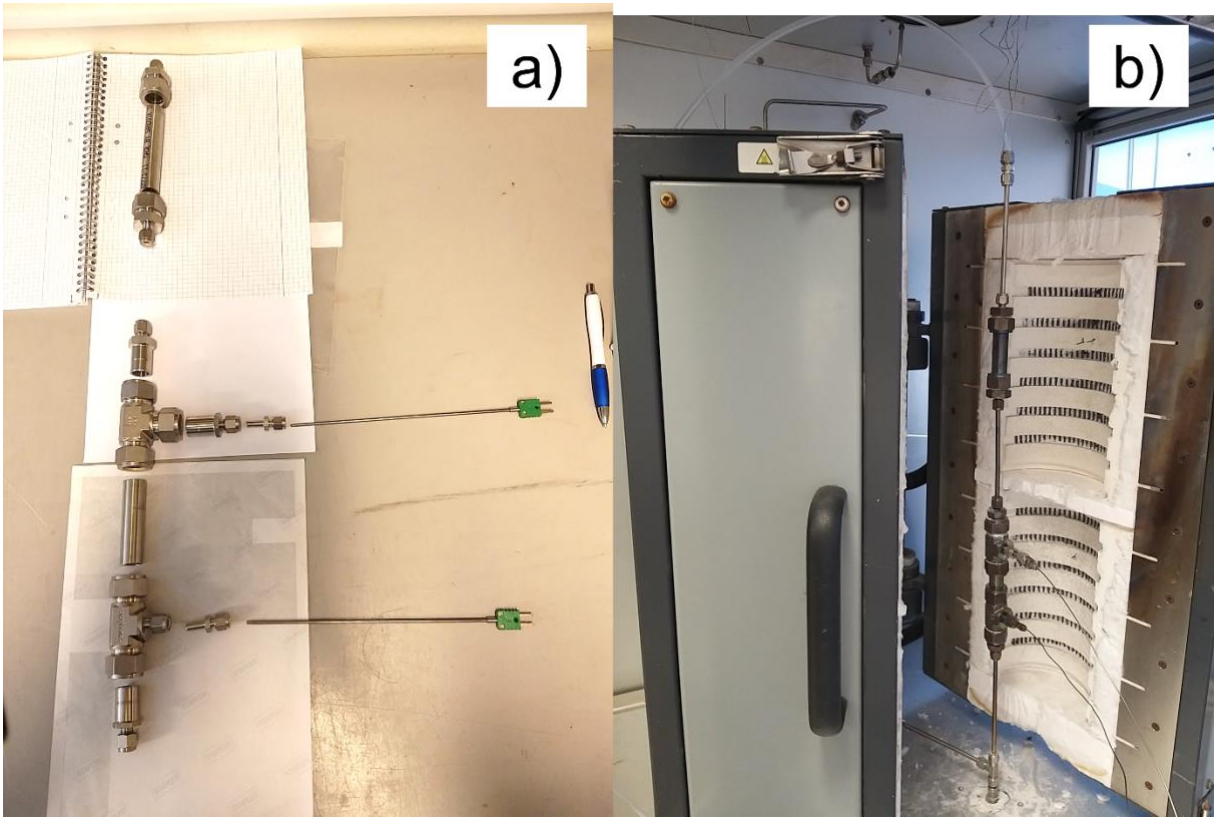

Figure 7.2. a) Reactor parts. b) Reactor inside the rig.

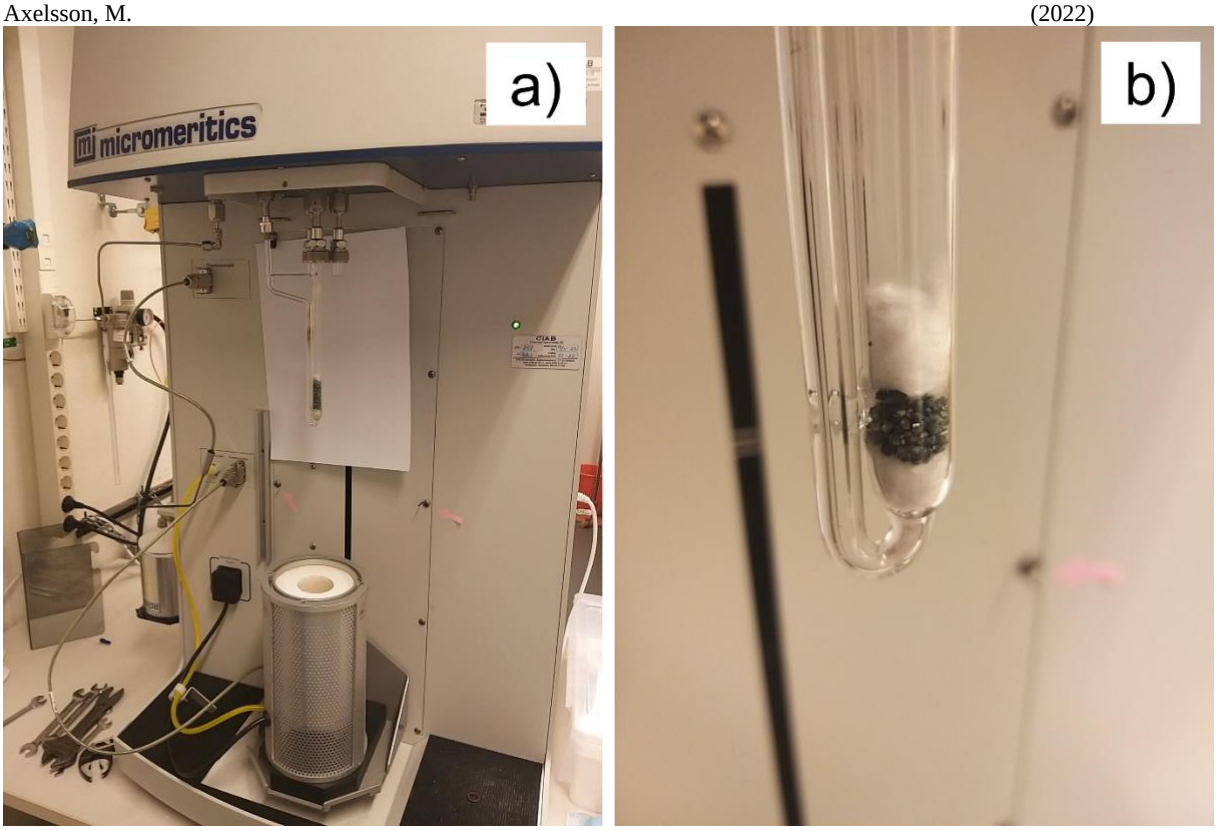

Figure 7.3 a) Micromeritics 3Flex analysis equipment. b) Quartz tube with catalyst sample.